High Resolution Investigation of Thermal Spatial Variability of Two Cobble Bed Rivers, and the Correlation to Salmonid Spawning Preferences

by

Cailey Ann Ellen McCutcheon

A thesis
presented to the University of Waterloo
in fulfilment of the
thesis requirement for the degree of
Master of Applied Science
in
Civil Engineering

Waterloo, Ontario, Canada, 2016

I hereby declare that I am the sole author of this thesis. This is a true copy of this thesis, including any required final revisions, as accepted by my examiners.

I understand that my thesis may be made electronically available to the public

Abstract

This thesis introduces and demonstrates the application of a recently designed mobile streambed temperature measurement system. The apparatus, called the High Resolution Temperature Mapping Device (henceforth HI-RES TMD) was built to increase the resolution of established temperature sampling methods and instantaneously acquire 32 equally distributed temperature measurements within 3 m^2 (0.3 m grid spacing) at the streambed interface. Sampling is done under wadable flow conditions, and can be completed every 4-5 minutes. This allows sampling of any spatial extent such as full morphological units or the reach scale within hours or days respectively. The HI-RES TMD is able to overcome many of the short comings of previous sampling methods such as the range of investigation of a given study, or require the insertion of temperature probes into the substrate which considerably increased sampling time. The HI-RES TMD has been field tested in two mountain streams located along the western slope of the Rocky Mountains, in southeastern British Columbia, Canada to examine temporal repeatability of thermal streambed patterns.

A dataset of more than 80,000 individual streambed temperature measurements was obtained using the HI-RES TMD. A series of analysis were then completed to determine whether the spatial variability of streambed temperature plays a role in the choice of spawning locations for fish. Both rivers are characterized by intense spawning of two salmonid species: cutthroat trout (*oncorhynchus clarkia*) and bull trout (*salvelinus confluentus*). This was confirmed during three consecutive seasons of spawning site surveys completed between 2012 and 2014 with the help of expert fisheries biologists at which time the precise locations of all the spawning locations (i.e., redds) within the study areas were surveyed. Analysis of streambed temperature patterns on the morphological features presented correlations between the average thermal distributions and spawning density and repeatability. Spatial autocorrelation analysis was completed to identify hot spots and cold spots within the study areas. It was found that bull trout redd density and repeatability were significantly correlated to the cold spots. As presence of colder areas on the streambed may be related to hyporheic flow or groundwater emergence, recommendations for improvements of the HI-RES TMD present an opportunity to determine if the bull trout redds are also correlated to groundwater emergence.

Acknowledgements

I would like to thank my supervisor Dr. William Annable for his guidance, support, and mentorship over the past years. Bill has provided the resources and opportunities to make this research possible, which has allowed me to further develop my passion for research and innovation. My desire to "find answers" was fueled by Bill's passion for river science which pushed me well beyond my comfort zone and helped me understand what I am truly capable of tackling, and for this I am extremely grateful.

This research required an extensive amount of field work, coordination and collaboration. I would like to acknowledge all the members of the Eco-Hydraulics Research Group (Ben Plumb, Lorenzo Brignoli, Jeff Muirhead, Brad Burrows, Chris McKie and Logan Koeth) for many hours of help with proof reading, field work and mental support. I would like to acknowledge the members of Trout Unlimited (Jack Imhof and Larry Mellors) and the staff at the Canadian Columbia River Inter Tribal Fisheries Commission (CCRIFC) (Bill Green, Will Warnock, Jon Bisset, Katrina Caley, JoAnne Fisher and Jim Clarricoate) who assisted with field work, shared equipment and provided council and guidance. A special thank you to Laura Bossers and Brad Burrows for following me across the country to live at the river banks and complete the majority of the field work for this thesis.

Thank you to the technicians in the Department of Civil and Environmental Engineering that patiently listened and accommodated most of my experimental ideas. Special thanks goes to Terry Ridgway who spent countless days helping and instructing me on electrical wiring, programing, surveying, trouble shooting and brain storming. Without Terry's help this equipment would have never left the drawing board, and for this I am extremely grateful.

This field work couldn't have happened without our ever gracious BC host and funding coordinator, Jon Bisset. Jon's passion for fisheries research and positive nature helped us overcome many logistical difficulties associated with field work, which he further entertained by sharing his house, and secret fishing locations for our redd surveys. It was very rewarding to work with such a passionate researcher and Jon's contributions are much appreciated.

I would like to thank the Department of Civil and Environmental Engineering, Teck Coal Limited, the Natural Science and Engineering Council of Canada Industrial Partnership Scholarship (NSERC-IPS) program, Ontario Graduate Scholarship (OGS) foundation, the Grand River Conservation Authority (GRCA), and CCRIFC, for providing the financial resources required for the completion of this research.

Dedication

This thesis is dedicated to my husband, Lorenzo Brignoli; your never failing love, encouragement and support helped me obtain new levels of discipline, knowledge and exhaustion needed to complete this thesis.

I would also like to dedicate this thesis in memory of my grandfather, Harold McCutcheon who passed in the summer of 2014.

Table of Contents

Abstract iii

Acknowledgements iv

Dedication v

List of Figures viii

List of Tables x

List of Appendices xi

List of Abbreviations xii

Chapter 1: Introduction 1
1.1 Thesis Structure 3

Chapter 2: High resolution streambed temperature data collection system 4
2.1 Introduction 4
2.2 Background 6
2.3 HI-RES TMD System 8
2.3.1 Temperature Calibration and Correction 10
2.3.2 Field Verification 11
2.3.3 HI-RES TMD Operations 12
2.3.4 Quality Control Measures 13
2.3.5 Temperature Normalization 14
2.4 Reproducibility of Streambed Trends 20
2.5 Conclusion 22

Chapter 3: Characteristics of Streambed Temperatures of Two Rocky Mountain Salmonid Spawning Streams. 23
3.1 Introduction 23
3.2 Background 25
3.3 Methods 28
3.3.1 Site Selection 28
3.3.2 Thermal Data Collection 33
3.3.3 Data Processing 36
3.3.4 Statistical and Spatial Analysis Methods 37
3.3.4.1 Bonferroni t-Test 37
3.3.4.2 F-Test 37
3.3.4.3 Least Significant Difference (LSD) Test 38
3.3.4.4 Spatial Autocorrelation (SAC) Analysis 39
3.3.4.5 Redd Proximity Metric 41
3.4 Results 43
3.4.1 Visual Analysis 43
3.4.2 Parameter comparison 47
3.4.3 Morphological Feature Statistical Population Comparison 51
3.4.4 SAC Analysis with Proximal Redd Spatial Correlations 61
3.5 Discussion 63
3.6 Conclusions and Recommendations 64

Conclusions 66
References 68
Appendices 77
Glossary 84

List of Figures

Figure 2-1: Schematic of HI-RES TMD (a) profile and (b) planform, and (c) field photograph. 9
Figure 2-2: Example of (a) temperature calibration (b) corrected temperature for one of the 33 Sensorex CS150TC-K probes within the HI-RES TMD system. 11
Figure 2-3: Field validation of temperature accuracy 12
Figure 2-4: Schematic example of HI-RES TMD operations from a) first cage data acquisition to b) and series of cages illustrating the transverse and upstream sequence of sampling. 13
Figure 2-5: Depiction of the spatial definition of cages and cross sections. 16
Figure 2-6: Post maps of measurement locations (a & b) with associated isotherm maps from (c & d) from July 2014 and September 2014 respectively, from a sub-reach of the Lizard Creek study site 21
Figure 3-1: Illustration of the salmonid spawning technique within a river setting. a) Pre-spawning stage; b) cutting; c) displacement of streambed material; d) transport of fine-grained sediment downstream; e) oviposition; f) covering of fertilized ova and subsequent upstream pit excavation (Marchildon 2009). g) Resulting well sorted bed material within the redd (Burner 1951). 30
Figure 3-2: Annual density, cumulative density and repeatability of redd surveys between 2012 and 2014 of a) Ram Creek and b) Lizard Creek study reaches. 32
Figure 3-3: Extents of thermal study reaches with surveyed redd locations for a) Ram Creek and b) Lizzard Creek. 35
Figure 3-4: Schematic illustrating how the redd proximity metric (R_i) is calculated for a representative redd 42
Figure 3-5: Isotherms of Ram Creek with magnified windows of interest 45
Figure 3-6: Isotherms of Lizard Creek with magnified windows of interest 46
Figure 3-7: Relationship between standardized temperature and flow depth for both study sites. Error bars show the standard deviation. 48
Figure 3-8: Relationship between standardized temperature and radiation for both study sites. Error bars show the standard deviation. 48
Figure 3-9: Relationship between standardized temperature and flow depth for both (a) Ram Creek and (b) Lizard Creek 50
Figure 3-10: Histograms of all the standardized temperature data collected on (a) Ram Creek and (b) Lizard Creek 51
Figure 3-11: Comparison of the redd annual density and ρ identifying the type of correlation to cold spots at Ram Creek. 62

Figure A. 1: Calibration curves for all 32 temperature probe within the HI-RES TMD, and the surface water control probe (labelled Probe 33) 79

Figure A. 2: Validation curves for all 32 temperature probe within the HI-RES TMD, and the surface water control probe (labelled Probe 33) 80

List of Tables

Table 2-1: Specification of HI-RES TMD sampling equipment 10
Table 2-2: Summary of tested normalization methods 17
Table 2-3: Conditions of the normalization equation 19
Table 2-4: Summary of data collected on Lizard Creek during investigation on the same sub-reach from July 21, 2014 and September 14, 2014. 21
Table 3-1: General morphological conditions of Ram Creek and Lizard Creek 29
Table 3-2: Summary of data collected on Ram Creek and Lizard Creek 34
Table 3-3: Summary of averages and variances of standardized temperature for each feature class 53
Table 3-4: Summary of statistical analysis completed on standardized temperature populations 54
Table 3-5: Summary of average thermal measurements, physical characteristics and spawning patterns at Ram Creek, sorted by average Z_{ijk} value. Features statically the same as the coldest feature are highlighted in blue and feature statistically the same as the warmest feature are highlighted in red. 57
Table 3-6: Summary of average thermal measurements, physical characteristics and spawning patterns at Lizard Creek, sorted by average Z_{ijk} value. Features statically the same as the coldest feature are highlighted in blue and feature statistically the same as the warmest feature are highlighted in red. 58
Table 3-7: Comparison of measurements within redds to the entire feature 59
Table 3-8: Summary of significant spot characteristics from both Ram and Lizard Creek 61

Table B. 1: Summary of redds observed on Ram Creek 82
Table B. 2: Summary of redds observed on Lizard Creek 83

List of Appendices

Appendix A: Temperature Probe Calibration and Validation Curves 78
Appendix B: Redd Survey Counts 81

List of Abbreviations

A_n	Planometric area of significant spots delineated with the SAC analysis
ANOVA	Analysis of variance
ARMA	Autoregressive Moving Average model
d	Maximum separation distance in which all other points are included within the calculation of G_i^*
E	Expected value (or geometric mean)
f_{obs}	Observed f-value statistic obtained from the F-Test
$f_{\alpha,df1,df2}$	Critical value of the F-Test
G_i^*	Getis-Ord statistic
l_n	Separation distance between the centroids of the significant spot n and the redd i
LSD	Least significant difference
p_{ijk}	Probability score for measurement i, cage j, and cross section k
Q^*	Net radiation energy flux
Q_a	Heat and advection energy flux from submerged flow
Q_b	Bed conduction energy flux
Q_e	Latent heat energy flux
Q_f	Frictional energy flux
Q_h	Sensible thermal energy flux
Q_O	Other thermal energy sources/sinks
R_i	Redd proximity metric
SAC	Spatial autocorrelation
T_{ijk}	Indexed temperature for measurement i, cage j, and cross section k
t_{obs}	Observed t-value statistic of the Bonferroni t-Test
$t_{\alpha/2}$	Critical value of the Bonferroni t-Test
Var	Variance
Z_{Gi*}	Standardized G_i^* value
Z_{ijk}	Standard temperature score for measurement i, cage j, and cross section k
α	Significance level
ρ	Cumulative redd density
ρ_A	Annual redd density
ρ_R	Redd repeatability

Chapter 1: Introduction

Spawning location preferences of salmonids have been well documented over the past several decades (White 1930; Burner 1951; Hale and Hilden 1969; Witzel and Maccrimmon 1983; Rieman and McIntyre 1993; Jonsson and Jonsson 2011; Eckmann 2014). Several abiotic metrics have been identified such as hydraulic properties (Lounder 2011; Marchildon et al. 2011; Marchildon et al. 2012), water quality (Hansen 1975; Ringler and Hall 1975; Geist 2000; Bickel and Closs 2008), riparian cover (Knapp and Preisler 1999; Zimmer and Power 2006), groundwater upwelling (White 1930; Hale and Hilden 1969; Witzel and Maccrimmon 1983; Rieman and McIntyre 1993; Jonsson and Jonsson 2011; Eckmann 2014), bed material grain size distribution (Kondolf and Wolman 1993; Baxter and McPhail 1997; Muhlfeld 2002; Mull and Wilzbach 2007), and thermal niches (White 1930; Hendricks and White 1988; Hannah et al. 2004; McMahon et al. 2007).

Numerous studies have acknowledged point source thermal habitat niches at the streambed interface as a selection criteria by many species of fish in choosing spawning locations and their subsequent construction of redds (Kondolf and Wolman 1993; Baxter and McPhail 1997; Muhlfeld 2002; Mull and Wilzbach 2007). Thermal habitat niches may result from different factors affecting streambed temperature variations at smaller scales. These include groundwater and hyporheic flow (Vaux 1967; Bencala 2000; Conant 2001) shading (Johnson 1971; Beschta 1997), thermal capacity of streambed material (Usowicz et al. 2006; Barry-Macaulay et al. 2015), aquatic vegetation (Buss et al. 2009) and, river confluencing (Chanson 2004) resulting in thermal habitat niches. Methods characterizing the general thermal characteristics of river systems can be found in literature (Stonestrom & Constantz 2003; Conant 2004; Dale & Miller 2007; Vogt et al. 2010) nevertheless, these methods are often characterized by low spatial resolution or do not encompass the whole extension of a river reach, rather focusing on spawning sites or other specific locations thus causing This thesis introduces and demonstrates the application of a recently designed mobile streambed temperature measurement system. The apparatus, called the High Resolution Temperature Mapping Device (henceforth HI-RES TMD) was built to increase the resolution of established temperature sampling methods and instantaneously acquire 32 equally distributed temperature measurements within 3 m^2 (0.3 m grid spacing) at the streambed interface. Sampling is done under wadable flow conditions, and can be completed every 4-5 minutes. This allows sampling of any spatial extent such as full morphological units or the reach scale within hours or days respectively. The HI-RES TMD is able to overcome many of the short comings of previous sampling methods such as the range of investigation of a given study, or require the insertion of temperature probes into the substrate

which considerably increased sampling time. The HI-RES TMD has been field tested in two mountain streams located along the western slope of the Rocky Mountains, in southeastern British Columbia, Canada to examine temporal repeatability of thermal streambed patterns.

A dataset of more than 80,000 individual streambed temperature measurements was obtained using the HI-RES TMD. A series of analysis were then completed to determine whether the spatial variability of streambed temperature plays a role in the choice of spawning locations for fish. Both rivers are characterized by intense spawning of two salmonid species: cutthroat trout (*oncorhynchus clarkia*) and bull trout (*salvelinus confluentus*). This was confirmed during three consecutive seasons of spawning site surveys completed between 2012 and 2014 with the help of expert fisheries biologists at which time the precise locations of all the spawning locations (i.e., redds) within the study areas were surveyed. Analysis of streambed temperature patterns on the morphological features presented correlations between the average thermal distributions and spawning density and repeatability. Spatial autocorrelation analysis was completed to identify hot spots and cold spots within the study areas. It was found that bull trout redd density and repeatability were significantly correlated to the cold spots. As presence of colder areas on the streambed may be related to hyporheic flow or groundwater emergence, recommendations for improvements of the HI-RES TMD present an opportunity to determine if the bull trout redds are also correlated to groundwater emergence.

spatial bias in the analysis (Hendricks and White 1988; Rieman and McIntyre 1996; Muhlfeld 2002). Furthermore, often these methods have been found to be highly time consuming and requiring extensive financial resources (Hendricks and White 1988; Conant 2004). Therefore, salmonid spawning location preferences assumptions are oftentimes based upon sparse thermal observations.

Consequently, it is still largely unknown whether salmonids select micro-scale thermal refugia or they are more generally attracted to macro-scale (i.e., reach scale) temperature regimes. Differentiation between these scales becomes particularly relevant in river restoration practices as the evaluation of anthropogenic impacts (such as water taking, mining, urbanization, etc.) on spawning habitats and subsequent measures of mitigation may vary widely at the spatial scale.

The development of a High Resolution Temperature Mapping Device (HI-RES TMD) allows a thorough and accurate characterization of streambed temperatures at small scales (0.09 m^2). Streambed temperature mapping was performed on two reaches located on two watercourses in southeastern British Columbia, Canada. Measurements were undertaken over the summer low-flow period of 2014 and spatially correlated to both cutthroat trout (o*ncorhynchus clarkii*) and bull trout (s*alvelinus confluentus*) redds surveyed between 2012 and 2014. A number of different statistical analyses were completed to determine

spatial correlations and causality between redds and micro-scale thermal refugia within both study reaches.

The main objectives of this work are the following:

i) Develop and deploy a streambed temperature measurement apparatus that is able to collect high spatial resolution data over a reach containing several morphometric features,
ii) Determine if a correlation exists between thermal spatial distribution of the streambed and the locations selected for spawning by salmonid species.

1.1 Thesis Structure

The format of this thesis follows a multi-part structure whereby Chapters 2 and 3 are organized into two distinct topics with respective introductions, methods, results, discussions, and conclusions, also known as manuscript format.

Chapter 2 introduces and demonstrates the High Resolution Temperature Mapping Device (HI-RES TMD); a streambed temperature measurement apparatus developed for this researched and designed for high resolution data collection. This Chapter presents the development process of the equipment and deployment on two rivers in southeastern BC and provides insight to the extent and resolution of data able to be capture by the HI-RES TMD and the accuracy of the equipment.

Chapter 3 examines the data collected during the deployment of the HI-RES TMD to analyze the correlation between the spatial thermal distribution of the streambed and salmonid spawning habitat also within the streambed. A series of statistical population comparison analysis and spatial autocorrelation analysis were completed to determine the correlation between morphological features and significantly warmer and colder locations within the study reach. This Chapter includes a discussion of hyporheic flow and groundwater emergence within the study areas, and presents comments on future use of the HI-RES TMD.

Conclusion, recommendations, and bibliography for the entire document follow Chapter 3. Two Appendices are included (A and B) which present the calibration and validation curves of the HI-RES TMD and the details of the redd surveys completed. The compendium of works presented herein is considered appropriate for the awarding of the degree of Master of Applied Science (M.ASc.) from the University of Waterloo.

Chapter 2: High resolution streambed temperature data collection system

2.1 Introduction

Spawning site (i.e., redd) selection preferences of salmonids have been well documented over the past several decades (White 1930; Burner 1951; Hale and Hilden 1969; Witzel and Maccrimmon 1983; Rieman and McIntyre 1993; Jonsson and Jonsson 2011; Eckmann 2014). Abiotic metrics include (but are not limited to) hydraulic properties (Lounder 2011; Marchildon et al. 2011; Marchildon et al. 2012), water quality (Hansen 1975; Ringler and Hall 1975; Geist 2000; Bickel and Closs 2008), riparian cover (Knapp and Preisler 1999; Zimmer and Power 2006), groundwater emergence (White 1930; Hansen 1975; Baxter and Hauer 2000; Hannah et al. 2004), bed material grain size distribution (Kondolf and Wolman 1993; Baxter and McPhail 1997; Muhlfeld 2002; Mull and Wilzbach 2007), and thermal niches (White 1930; Hendricks and White 1988; Hannah et al. 2004; McMahon et al. 2007). Each of these process are also known to occur at nested spatial scales from the reach, morphological feature (i.e., pools/riffles/runs), mixing zone, bed material sizes, and down to the limits of the boundary layer (Stallman 1965; Vaux 1967; White et al. 1987; Muhlfeld 2002; Brown and Hannah 2008).

Several methods exist to characterize the general thermal characteristics of river systems such as spot measurements with thermometers or thermistors to continuous measurements using systematic data collectors coupled to thermistors to characterize storm, diurnal and seasonal variations in temperature (Stamp et al. 2013, Preud'homme and Stefan 1992). However, few methods exist to discretely measure streambed temperatures at the redd and smaller scales (Hendricks and White 1988; Conant 2004). These methods have also proven to be highly laborious thereby restricting the spatial extents of a given study. Of those investigating redds, spatial bias has been common place as most measurements are obtained within redds with few (if any) beyond their limits (Hendricks and White 1988; Rieman and McIntyre 1996; Muhlfeld 2002).

This paper introduces and demonstrates the application of a recently designed streambed temperature measurement system which expands upon established methods at increased spatial resolution. The device is able to instantaneously acquire 32 temperature measurements within 3 m^2 (0.3 m grid spacing) at the streambed interface, under wadable flow conditions, and can complete a sampling interval every 4-5 minutes, which allows for sample of full morphological units to the reach scale within hours to days respectively. The system has been field tested in addition to being deployed in a mountain stream in

southeastern British Columbia, Canada (western slope of the Rocky Mountains), to examine temporal repeatability of thermal streambed patterns. The instantaneous measurement of streambed temperatures at multiple locations in close proximity is able to overcome previous sampling limitations of the range of investigation of a given study, or require the insertion of temperature probes into the substrate which considerably increased sampling time.

2.2 Background

Over the past several decades, many temperature monitoring technologies have been developed and made publicly available for river temperature monitoring. While these technologies have been developed to reduce much of the labor and time associated with field data collection, handicaps remain which limit their ability to collect high resolution streambed temperatures at the morphologic unit or reach-scale. Stand-alone continuous sampling thermometers have become inexpensive which can be deployed individually or integrated into other monitoring equipment (e.g., pressure transducers, water quality samplers, etc.). By distributing multiple devices at the sub-reach scale, time series of spatial temperature data can be acquired. However, the number of sensors required to examine spatial distributions of streambed temperatures in high resolution renders the approach cost prohibitive and highly subject to destruction from floods or vandalism.

Fibre optic cables are able to obtain both high frequency and resolution temperature measurements which have been deployed to monitor longitudinal changes in streambed temperature (Selker et al. 2006; Collier 2008; Vogt et al. 2010). However, deployment of these devices to investigate fine-scale longitudinal and transverse temperatures would require extensive lengths of cable and a secondary systems to georeference the sampling locations along each cable rendering the method cost prohibitive. Since the cables are also lain on or affixed to the bottom of the stream bed, they are also vulnerable to vandalism or being washed away during floods.

Infrared thermal imaging is becoming more accessible to monitoring temperatures in a non-invasive and timely fashion where spatial extents can be further enhanced by aerial equipment - such as aerial drones. However, thermographic cameras can only measure the infrared radiation emitted at the atmospheric interface (Yilmaz et al. 2003; Duarte et al. 2006; Burkholder et al. 2008), therefore restricting the cameras ability to obtain submerged temperatures and rendering this method inapplicable for this application.

The most common method used to acquire measurements at sub-meter resolution are georeferenced subsurface temperature measurements below the streambed interface. Temperatures are commonly measured at depths of approximately 10–20 cm (Hendricks and White 1988; Constantz 1998; Malcolm et al. 2003; Conant 2004; Kalbus et al. 2006). Submerged measurements reduced diurnal fluctuations and thermal mixing at the streambed interface (Kim et al. 2014) allowing for the spatial comparison of measurements with limited post–processing efforts (Hendricks and White 1988; Malcolm et al. 2003; Conant 2004). This approach is labour intensive which limits the spatial extent of a given study (Hendricks and White 1988; Conant 2001) and is also subject to frequent destruction of equipment

resulting from their often awkward insertion through the substrate. The method also differs by obtaining measurements directly at the streambed interface where salmonids are selecting spawning locations.

2.3 HI-RES TMD System

The High-Resolution Temperature Mapping Device (HI-RES TMD) was developed to measure high resolution streambed temperatures while overcoming several other common constraints of field investigations. The equipment is non-invasive (i.e., does not disturb the natural conditions being monitored), mobile, rugged and can work in most riverine settings under wadable flow conditions. A founding assumption of the sampling system outlined here is that measurements are obtained at the streambed interface where salmonids are scanning the river bed and choosing locations for spawning. Although submerged streambed measurements have successfully defined the spatial variability of the advective thermal energy caused from groundwater and hyporheic flow emergence (Hendricks and White 1988; Muhlfeld 2002; Malcolm et al. 2003; Conant 2004), other forms of thermal energy flux (i.e., sensible heat, latent heat, radiation, frictional energy and thermal conduction of the bed materials) affect the thermal distribution of the streambed temperatures (Caissie 2006; Hannah et al. 2008) and this method present here is able to capture, without bias, all the parameters affecting thermal spatial variability of the streambed interface where spawning habitat is selected. By instantly acquiring 32 thermal measurements within 3 m^2, which is a similar scale to a redd, subtle spatial differences in streambed temperature can be observed without temporal lag effecting the proximal measurements.

The apparatus incorporates 32 temperature probes, spaced 0.3 m apart in a planometric grid pattern (Figure 2-1). Constructed from aluminum, the apparatus is approximately 1.2 m wide by 2.5 m in length. This resolution produced the densest configuration of the temperature probes (maintaining compatibility with the datalogging equipment) at a size that could be easily managed by two operators. Total station prism mounts were designed into the four corners of the frame to geospatially locate the apparatus: in this case a Trimble Robotic S6 total station (±2 mm, Trimble Navigation Ltd. (2013)) was used. By georeferencing the four corners of the frame, the spatial coordinates of each probe can subsequently be determined. An additional temperature probe is located in the middle of the frame to acquire measurements at the midpoint flow depth. These data were obtained to assist with the comparisons between the 32 streambed point measurements and provide average characteristics of the surface water. A pyrometer was included on the top of the frame to measure incoming solar radiation which could be used to quantify thermal effects of shading from overhanging trees or cloud covered days. A staff gauge was located on one vertical leg so that bathymetry could be mapped from the associated total station prism mount location above. All sensors were connected to a single datalogger which could be downloaded via a wired computer connection. A custom computer code was developed to execute a thermistor calibration and data acquisition routine at each grid position. Additional MATLAB™ post-processing scripts were

developed to concatenate all the data into a single database. Table 2-1 lists the specifications of the measurement equipment used to collect all the above mentioned parameters.

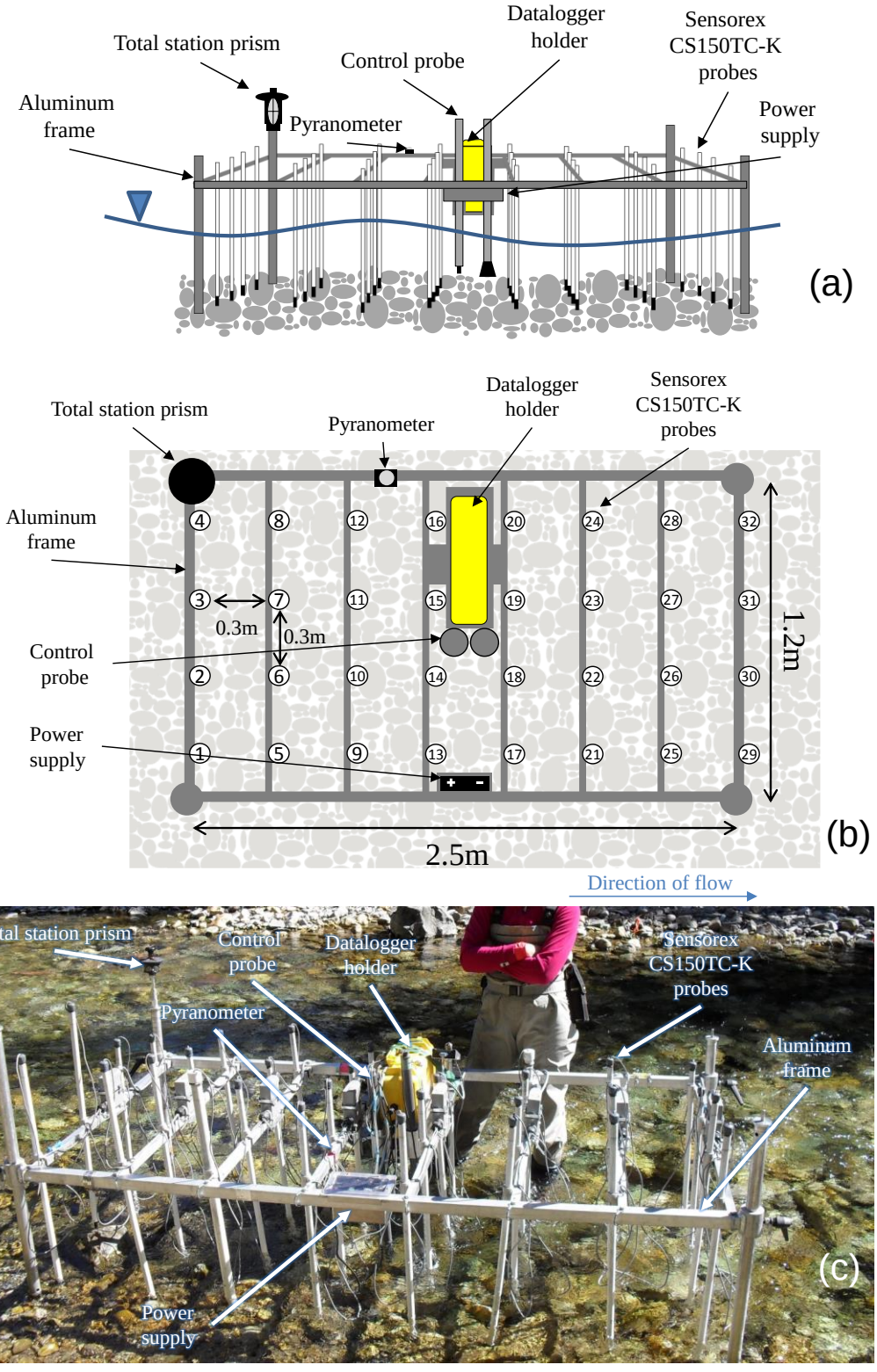

Figure 2-1: Schematic of HI-RES TMD (a) profile and (b) planform, and (c) field photograph.

Table 2-1: Specification of HI-RES TMD sampling equipment

Parameter	Measurement Device	Comments			
Datalogger	Campbell Scientific CR1000 with CR1000-KD (keyboard and display)	• Powered by and external 12V battery • Transfer of data to computer was completed using Direct Read (Serial to USB) • Sample rate is determined by user (for all parameters)			
Parameter	**Measurement Device**	**Method of Recording**	**Sampling Range**	**Accuracy**	**Resolution**
Temperature	Sensorex CS150TC-K	Automatically recorded into the datalogger	0-70°C	0.01°C	0.01°C
Radiation	Unknown (refurbished equipment)	Automatically recorded into the datalogger	0–2.0 kW/m^2	0.01 kW/m^2	0.01 kW/m^2
Flow Depth	In-house made gauging rod	User input to datalogger	0-0.8 m	0.01 m	0.02 m
UTM Coordinates	Trimble S6 Total Station	Trimble Datalogger	150 m	0.001 m	0.001 m

2.3.1 Temperature Calibration and Correction

Temperature probes were calibrated using a thermal bath (Steinhart and Hart 1968; Sabatino et al. 2000). All probes were placed in the bath at the same time and a three-point temperature calibration was performed. Temperatures of 8°C, 16°C, and 22°C were selected for the calibration as this captured a common range of streambed temperatures for southeastern BC (Moore 2006; Moore et al. 2013). Each probe recorded 50 consecutive measurements and the average of the measurements for each probe calculated and used for calibration purposes. A linear relationship between each average measured probe temperature and actual temperature was calculated (Figure 2-2(a)). Figure 2-2(b) shows the corrected temperature comparison for one probe between the probe corrected and actual temperatures after the correction was applied. The remaining calibration curves are included in Appendix A. Validation tests were completed 2-3 times a year to ensure the accuracy of the calibration was maintained over time; however no temporal drift was identified during any of the tests.

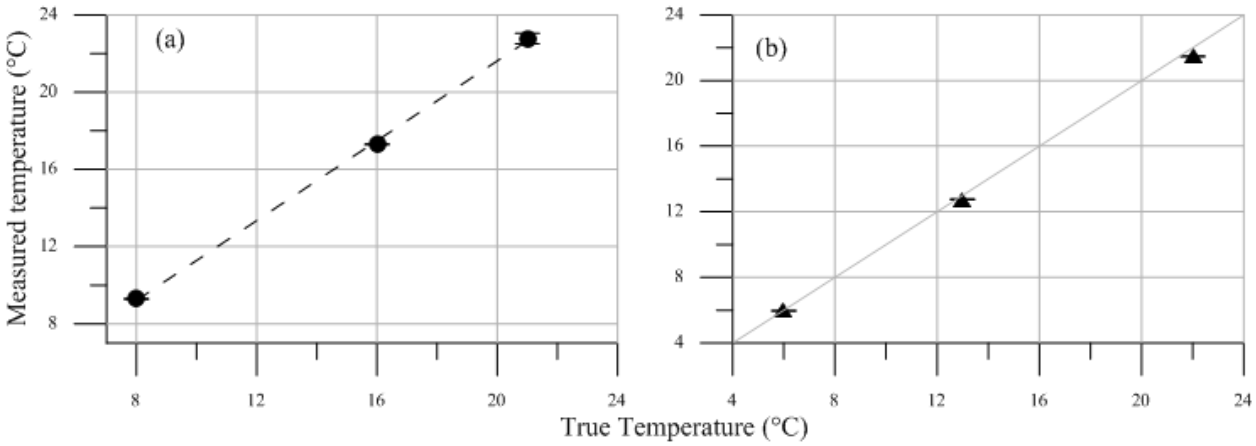

Figure 2-2: Example of (a) temperature calibration (b) corrected temperature for one of the 33 Sensorex CS150TC-K probes within the HI-RES TMD system.

2.3.2 Field Verification

The probes were confirmed to be measuring in the field with the same accuracy as during the laboratory calibration process. During field tests, an external digital thermometer (Fisher Scientific, model number T53, 0.1°C resolution) was used to measure the streambed temperature at the same location as one of the probes within the HI-RES TMD system. This external test was undertaken at the start of every second or third day to ensure temperature drift in sensor readings was not occurring. Tests identified that calibrated sensor readings were all within ±0.1°C of the external thermometer (Figure 2-3). While these observations are an order of magnitude lower in accuracy than in the laboratory calibration (±0.01°C), observed error is more than adequate for field applications given additional environmental variability.

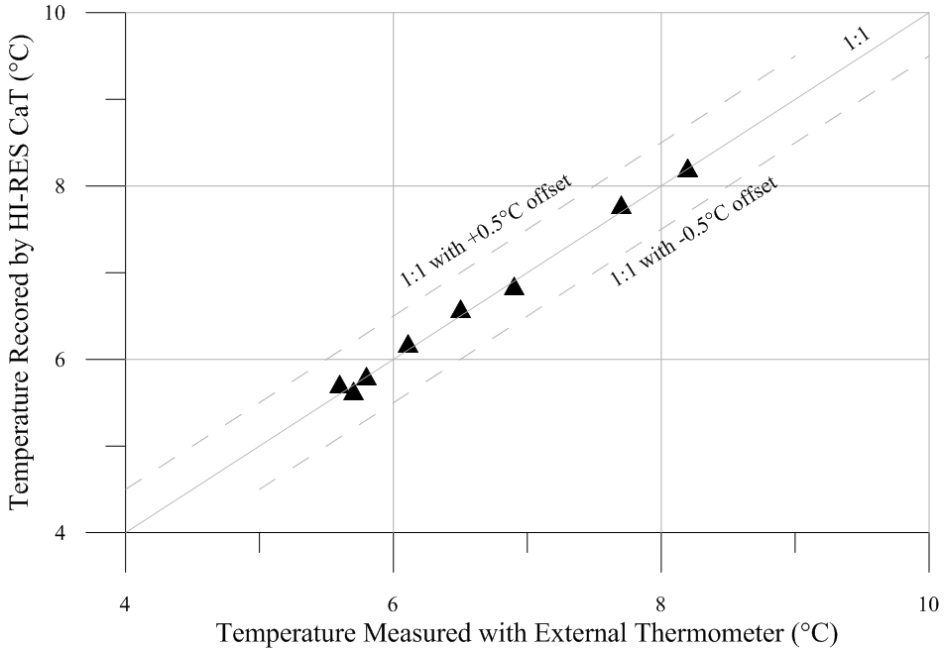

Figure 2-3: Field validation of temperature accuracy

2.3.3 HI-RES TMD Operations

Sampling with the HI-RES TMD begins by carrying the assembled equipment to the river and lowering the apparatus to the streambed. The frame is then levelled to allow all the temperature probes to rest on the streambed and the four corners of the frame are geospatially referenced employing the total station (by moving the total station prism to each of the four prism mounts). The flow depth is noted from the one vertical leg furnished with a one centimeter accurate staff gage. The mid-depth probe (control probe) is adjusted to the appropriate level. The operator then starts the recording of the HI-RES TMD by entering the flow depth into the datalogger and triggering the remaining measurements (channel bed temperature measurements, water column temperature and radiation), which are collected and recorded automatically into the data logger and the sampling sequence is completed. This sequence is subsequently referred to as a *cage* data acquisition.

The HI-RES TMD frame is then moved to an adjacent position and the sampling procedure repeated throughout each day of field investigation. The sequence of movement is in a transverse-longitudinal fashion to obtain a grid-like distribution of measurements moving in an upstream direction (Figure 2-4).

Recognizing that the spatial extents of each reach being investigated may require multiple days of HI-RES TMD sampling, diurnal and other temporal changes in water temperature may be required. An independent monitoring station was established upstream of the study reach and left in place for entire

duration of the investigation. In this case, a YSI 600OMS V2 Optical Monitoring Sonde (equipped with temperature), a HOBO pyranometer (recording radiation) and two HOBO 13-Foot Freshwater Level Data Loggers (to measure fluctuations in water level and to correct for changes in barometric pressure) were deployed sampling at 10 minute intervals. Parameters measured were used to assist in normalizing temperature data for both daily and study duration periods.

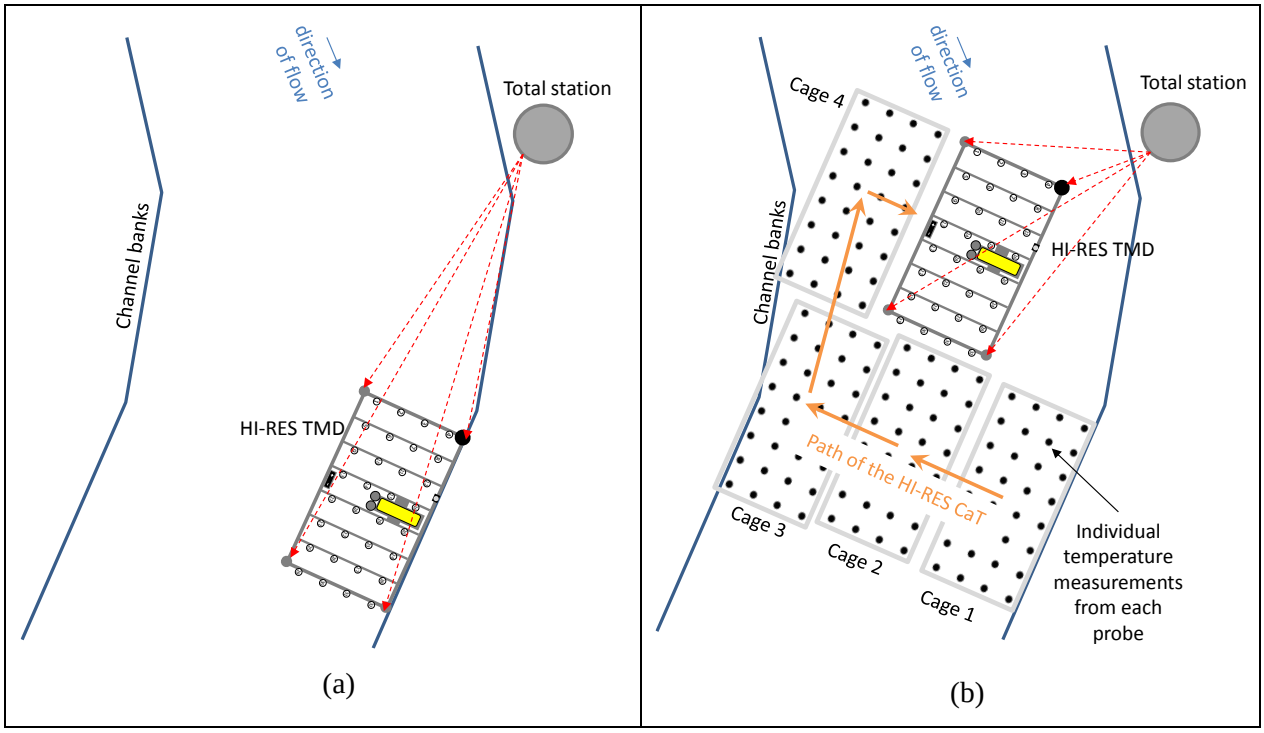

Figure 2-4: Schematic example of HI-RES TMD operations from a) first cage data acquisition to b) and series of cages illustrating the transverse and upstream sequence of sampling.

2.3.4 Quality Control Measures

Several quality control checks were implemented to ensure the accuracy of the equipment and data. Furthermore, additional complications and errors occurred during field campaigns, common to most field investigations, which resulted in the removal of additional data.

To ensure that the recorded measurements were representative temperatures, an equilibrium check was conducted during each cage measurement. The equilibrium check rapidly sampled temperatures from each of the 32 probes, and would report to the operator when the last three consecutive measurements, for each of the probes differed by less than 1% relative to each probe measurement. This test was conducted

at every new position of the HI-RES TMD system where the operator was required to wait until the equilibration test was complete before initiating data logging.

During each sampling sequence, every probe was inspected to ensure it was resting on the channel bed (i.e., not resting on obstructions such as tree branches or boulders that weren't fully submerged). The principle concern was that probes would be recording air temperature (i.e., resting above the water surface) which could be several degrees warmer or colder than the water temperature. A secondary concern arises where probes are not recording at the streambed interface which may also differ from the temperatures that the fish experience during the spawning. If the location of a probe could not be adjusted to rest of the channel bed, the discrete probe measurement was recorded as an "ERROR" and not used in any subsequent analysis.

It was possible that some probes were overlooked in the field, and might not have been touching the channel bed during the field operations. A secondary test was conducted during post-processing where a time series comparison to the independent temperature monitoring station (in this case the YSI 600OMS Sonde) was conducted. Any streambed temperature measurement that differed by more than 5°C above or below the daily recorded Sonde maximum or minimum water temperature respectively was parsed from the data set.

Initial data processing identified electronic malfunctioning of probes 9, 13, 15, 24, and 25. Due to the randomness of the error, all data from these probe was subsequently removed. Figure 2-1(a) illustrates the numbering sequence of the temperature sensor probes onboard the HI-RES TMD system.

2.3.5 Temperature Normalization

Diurnal fluctuations within the streambed temperatures were observed at both study sites therefore spatial comparison of the temperatures was not possible until the temporal variability was removed from the data.

As explained, previous spatial investigations of streambed thermal variability have avoided post processing and correction of diurnal fluctuations by collecting temperatures from the shallow subgrade of the streambed (Hendricks and White 1988; Malcolm et al. 2003; Conant 2004). Vertical temperature profile analysis has shown that the diurnal fluctuations of the streambed temperatures have a smaller range than that of the surface water, but a larger range than the temperatures within the shallow subgrade (Kim et al. 2014). However, this research focused on spawning selection preferences correlation to the thermal regimes that the fish are able to experience, therefore it was necessary to understand the thermal variability within the habitat zone. Therefore measurements were taken at the streambed, knowing that temperature normalization would be required for spatial comparison.

Several methods of normalization were attempted to create the most continuous and coherent dataset for comparison (Table 2-2). A series of finite-differencing techniques using autoregressive moving average models (ARMA), were derived calibrated and verified using the data collected from field investigations. Finite differencing is a common analytical technique used to remove underlying temporal trends within data (Hipel and McLeod 1994) and is a preferable solution as the units of measurement are maintained and the resulting metric is an easily conveyable parameter. Here, temporal-based ARMA models were employed (Hipel and McLeod 1994), however, the finite-differencing techniques were not able to capture the diurnal variance within the multi-day field measurements.

In order to employ standardized normalization techniques, moving window schemes were employed. This is a common analytical technique used to define diurnal variance within the measured range in field temperatures (Wójcik and Buishand 2003; Stisen et al. 2007; Zakšek and Oštir 2012). Through a series of trial-and-error attempts, it was found that the moving window needed to incorporate the full width of the river, as longitudinal transverse patterns of temperature were identified. A space for time substitution was employed, to define the limits of a moving window which was found to coincide with five cross sections of cages. Figure 2-5 illustrates cage locations and the limits of the moving window. Temporal thresholds were imposed on the size of the moving window to ensure that an appropriate amount of the diurnal trend was excluded within each moving window. Consequently, the number of cross sections included in the moving window was reduced if the elapsed time between cross sections was greater than 50 minutes.

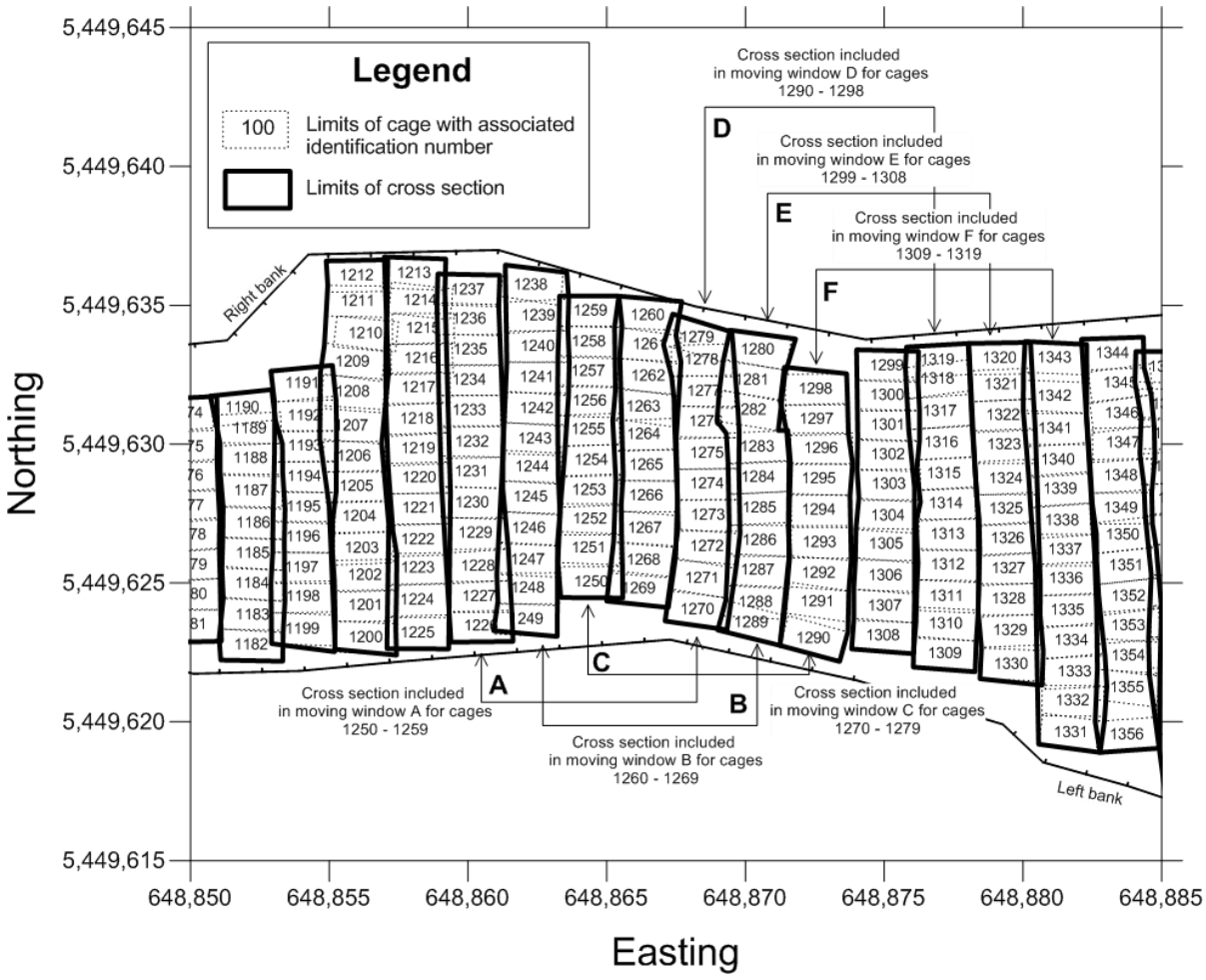

Figure 2-5: Depiction of the spatial definition of cages and cross sections.

Feature scaling (line 5, Table 2-2) was initially examined, producing a normalized temperature ranging between 0 and 1. Feature scaling is commonly used for data processing to reduce the range of values, and to allow for coherent comparison of parameters (Mohamad and Usman 2013); however, this process assumes that the range of the sample is representative of the variance, which was not a valid assumption for this dataset.

Table 2-2: Summary of tested normalization methods

	Definition of the normalized parameter	General Equation	Reasons for Exclusion From Analysis
1	Finite-differencing of the measured temperatures and an ARMA model of the Sonde temperatures	$\Delta T_{it} = T_{it} - T_t^{Sonde}$	This method created larger normalized differences at the start of the day and smaller differences at the end of the day. It was expected that the Sonde was subject to different warming trends than the probes on the HI-RES TMD.
2	Finite-difference of the measured temperatures and an ARMA model of the spatial dependent surface water temperatures.	$\Delta T_{ij} = T_{ij} - T_j^{SW}$	Similar to the Sonde differencing scheme, the diurnal trends of the surface water were not representative of the streambed. This was identified with significantly colder normalized differences at the start and end of each day.
3	Finite-difference of the measured temperatures and an ARMA model of cage average temperature	$\Delta T_{ij} = T_{ij} - \frac{1}{n}\sum_{\alpha=1}^{n} T_{\alpha j}$	This method was too site specific as the HI-RES TMD only covers an area of 3m^2. This removed too much of the spatial variability as the range of measurements within a single use of the HI-RES TMD was very small.
4	Finite-difference of the measured temperatures and a moving window ARMA model of cage average temperature	$\Delta T_{ij} = T_{ij} - \frac{1}{5}\sum_{\beta=j-2}^{j+2}\frac{1}{n}\sum_{\alpha=1}^{n} T_{\alpha\beta}$	Time restrictions were incorporated into this averaging. Cages *j-2, j-1, j+1* and *j+2* had to be completed within 40 minutes (20 minutes before and 20 minutes after) of cage *j*. If these time limits were exceeded the moving window was truncated to include only the measurements within the time frame. This method was also too site specific, which made temperatures outside of the standard deviation significant outliers.
5	Feature scaling using a five cross section moving window	$T'_{ijk} = \frac{T_{ijk} - T_{min}}{T_{max} - T_{min}}$	The range of the moving window was not a consistent representation of the variance of the moving window, muting the volume of extreme values.

Definitions:
$\Delta T_{measurement,time/cage}$ = Normalized temperature parameter
T_t^{Sonde} = temperature of the YSI Sonde at time *t*
T_j^{SW} = the surface water temperature recorded during cage *j*
T_{min} = the minimum temperature in the moving window
T_{max} = the maximum temperature in the moving window

In order to incorporate the irregularity of the variance, a standard score normalization was used for the previously defined moving window. A standard score represents the number of standard deviations of each value from the average of the sample which can also be presented as the probability of any temperature within the moving window being less than that of the sample (Mohamad and Usman 2013). As sample sizes (n) within the moving windows were greater than 30, a Gaussian distribution standard score was employed instead of a t-Distribution (Walpole et al. 1993). This method was able to provide the necessary fluidity of the data, and identify values that varied from the mean of the moving window.

The normalization values of standard score (Z_{ijk}) and probability (p_{ijk}) were defined as (Mohamad and Usman 2013):

$$Z_{ijk} = \frac{T_{ijk} - \mu_{MW}}{\sigma_{MW}} \qquad \text{where } -\infty \leq Z_{ijk} \leq \infty$$

$$p_{ijk} = \frac{1}{\sigma_{MW}\sqrt{2\pi}} \cdot e^{\frac{-(T_{ijk}-\mu_{MW})^2}{2\sigma^2}} \qquad \text{where } 0 < p_{ijk} < 1$$

respectively, where:

$$\mu_{MW} = \frac{1}{5}\sum_{\gamma=k-2}^{k+2}\frac{1}{m}\sum_{\beta=1}^{m}\frac{1}{n}\sum_{\alpha=1}^{n} T_{\alpha\beta\gamma} \ \ (gemetric\ mean\ of\ the\ moving\ window)$$

$$\sigma_{MW} = \sqrt{\sum_{\gamma=k-2}^{k+2}\sum_{\beta=1}^{m}\sum_{\alpha=1}^{n}\left(T_{\alpha\beta\gamma} - \mu_{MW}\right)^2} \ \ (standard\ deviation\ of\ the\ moving\ window)$$

and T_{ijk} is the indexed temperature measurement for measurement i, of cage j and cross section k (which is comprised of m cages where each cage has n measurements).

Additional constraints to the moving window excluded two separate days from being included within the same window as the temporal gap between these data points was too large. This issue arose because the last cross section of the day was spatially and temporally adjacent to the first cross section of the day. An additional anomaly was identified within the first cross section of measurements at the beginning of each day where the HI-RES TMD did not equilibrate to streambed temperatures prior to sampling. To account for this equipment bias, the first cross section of the day was normalized with an average of probe measurements exclusive to that section.

A further constraint was placed upon the analyses if the sampling duration became extended (such as additional time expended to circumnavigate obstacles or deep pools, operator breaks etc.) resulting in too

much diurnal variation being captured in the moving window. Through the calibration process, 50 minutes was determined to be the maximum acceptable time to complete a cross section and therefore specified as the sampling duration constraint. When exceeded, the sampled cross section was treated consistent with the method employed at the first cross section of the day using the average cross section measured temperature. Table 2-3 lists the final normalization constraints employed in the post processing of the temperature data.

Table 2-3: Conditions of the normalization equation

Condition	**Normalization Equation**
If *k* is equal to the first cross section of the day then	$\gamma \equiv k$
If *k* is equal to the second cross section of the day then	$\gamma \in [k, k+2]$
If *k* is equal to the third cross section of the day then	$\gamma \in [k-1, k+2]$
If *k* is equal to the second last cross section of the day then	$\gamma \in [k-2, k+1]$
If *k* is equal to the last cross section of the day then	$\gamma \in [k-2, k]$
If the time require to complete a cross section, or the duration of the time between cross sections is $t \geq 50$ min then	Cross section treated as first cross section of the day; therefore $\gamma \equiv k$ Surrounding cross sections were also treated accordingly (i.e., previous cross section was treated as the last of the day, the following cross section was treated as the second of the day, etc.)

2.4 Reproducibility of Streambed Trends

The HI-RES TMD system was deployed along the same 15 m sub-reach of Lizard Creek located 5 km south of Fernie, BC on July 21st and September 14th of 2014. Lizard Creek is a gravel-bed channel with an average bankfull width, banfkull depth, channel slope and sinuosity of: 9.3 m, 0.6 m, 0.9% and 1.2 respectively. The alpine watershed is relatively undeveloped with some logging over the past 150 years and is known by several professional aquatic biologists to be a highly productive cutthroat trout spawning stream (Jon Bisset, Canadian Columbia River Inter-Tribal Fisheries Commission, per. Comm). There were several differences between the external environmental conditions during the two sampling periods (Table 2-4), with the most notable being the air temperature, which averaged 22 °C on July 21st and 10 °C on September 14th. The streambed temperatures only differed by approximately 3°C between the two sampling periods. Results of the spatial distribution in streambed temperature measurements and standardized temperature results for both study days are illustrated in Figure 2-6.

Both the July and September isotherms produced similar standardized temperature patterns; the most easterly region being cooler with the temperature increasing in a westerly direction, and decreasing again at the most westerly (upstream) extent. Both investigations were able to capture the location and extent of the isolated cold area (**C**) along the central left bank and the isolated warm (**H**) location along the westerly left bank (Outlined with rectangles in Figure 2-6.). The cold location identified was noted as the only spot within the sub-reach with vegetation in the channel. It is possible that at this location, vegetation is providing sufficient shading to reduce the thermal capacity (Johnson 2004) of the channel at this location or that the roots of the vegetation are creating preferential pathways for groundwater emergence within the channel at this location (Buss et al. 2009; Stubbington et al. 2009). Further field investigations would be required to determine the specific cause of the isolated thermal variability.

The similarity of the patterns indicates that the HI-RES TMD equipment was able to reproduce the results within the same low flow season and worked consistently throughout the duration of the field investigations. Furthermore as the magnitudes of the isotherms were of similar values, this indicates that the standard score normalization was able to effectively remove the diurnal trends. The July investigation was completed during a more variable, warmer temperature range, and was collected over a longer duration than the September data collection (Table 2-4). The standardized data was able to show approximately the same results despite the limited consistency between the July and September external boundary conditions. It is noted that the isotherm map from September has somewhat more detail than the July map: n = 1536 versus n = 1280 respectively. It is possible that the lower sampling resolution in the July campaign resulted in the more uniform distribution in temperatures (Figure 2-6 (c)) versus the

September sampling campaign (Figure 2-6(d)); particularly within the most downstream portion of the study sub-reach.

Table 2-4: Summary of data collected on Lizard Creek during investigation on the same sub-reach from July 21, 2014 and September 14, 2014.

Parameter	July 21, 2014	September 14, 2014
Total number of streambed temperature measurements	1280	1536
Total number of measurements post error removal processing	1184	1521
Hours of sampling	12:50 PM–6:10 PM	1:50 PM–4:10 PM
Range in streambed temperatures (difference in brackets)	10.49°C-13.26°C (2.77°C)	7.99°C-9.93°C (1.94°C)
Standard deviation in streambed temperatures	0.67°C	0.35°C
Range in flow depths	0.03-0.57	0.01-0.52
Range in atmospheric temperatures	20.6°C-23.2°C	7.68°C-12.11°C
Range in radiation during investigation	0.13V–1.45V	0.04V–1.14V

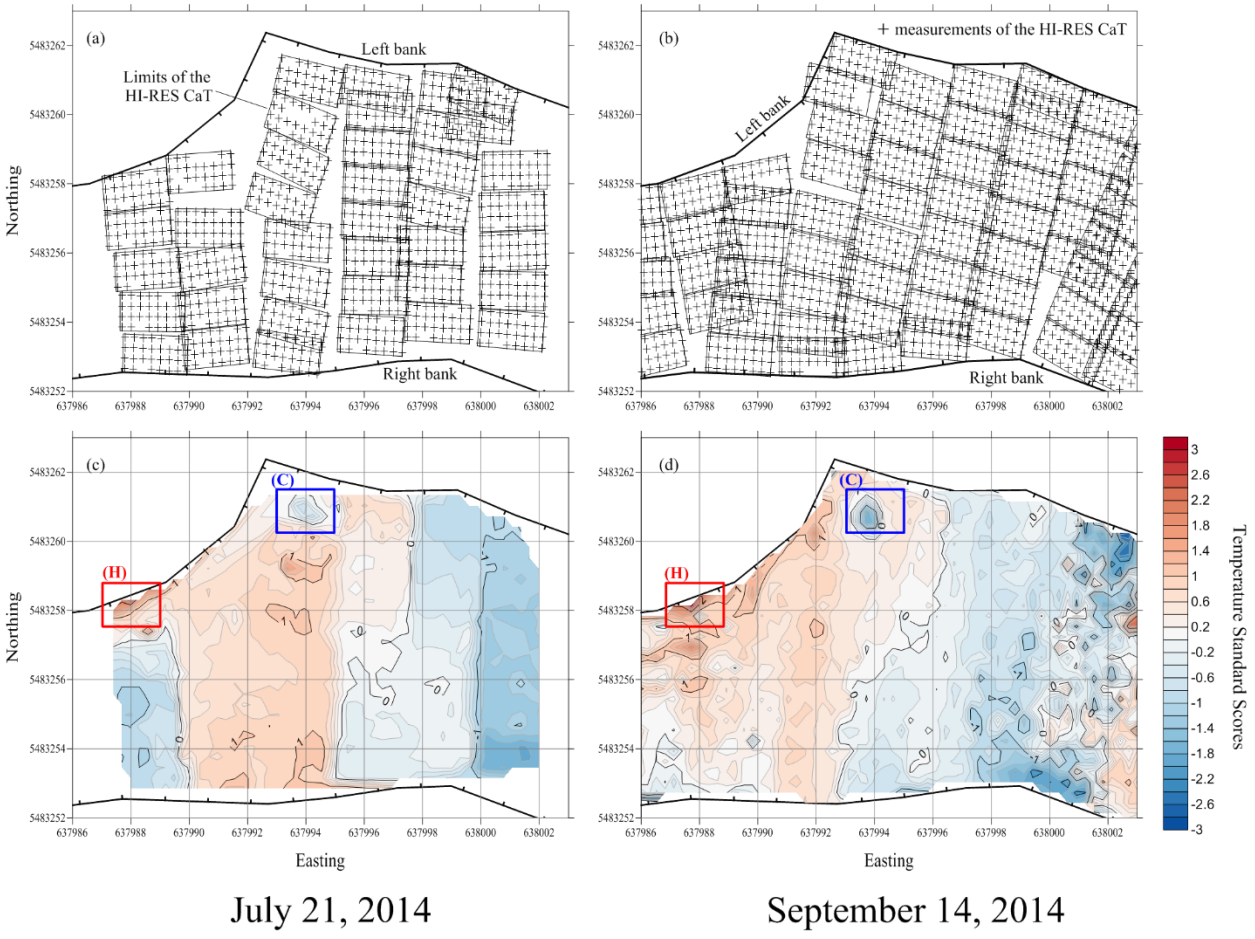

Figure 2-6: Post maps of measurement locations (a & b) with associated isotherm maps from (c & d) from July 2014 and September 2014 respectively, from a sub-reach of the Lizard Creek study site

2.5 Conclusion

The HI-RES TMD system was developed to sample streambed interface temperatures in high resolution. The equipment was designed for, and employed during, low flow wadable stream conditions where multiple morphologic units can be sampled in a single day (depending on river scale) in unprecedented resolution During its deployment, no negative impacts to aquatic habitat occurred as a result of the sampling method.

While it was necessary to create a normalized metric for the data analysis, a standard score metric with associated probability allowed for seamless comparison of the entire datasets. The data was able to be spatially plotted arising from the georeferenced positing of each monitoring probe and compared using the standardized temperature score. The effectiveness of the normalization equations accommodated the reduced efforts associated with the HI-RES TMD data collection.

Chapter 3: Characteristics of Streambed Temperatures of Two Rocky Mountain Salmonid Spawning Streams.

3.1 Introduction

Stream temperature is considered by many aquatic ecologists and biologists to be a central metric for assessing and categorizing the aquatic health of lotic ecosystems (Meyer 1997; Bunn et al. 1999; Feio et al. 2010). Water temperature is primarily governed by the non-point source conditions of latitude and elevation where relatively systematic modulations occur at both seasonal and diurnal time scales. Reach scale and point-source scale temperature modulations can also occur as influenced by groundwater outflow, hyporheic flow, both atmospheric and terrestrial shading, thermal capacity of streambed material, aquatic vegetation and, river confluencing (Stallman 1965; Vaux 1967; Caissie 2006; Hannah et al. 2008; Vogt et al. 2010; Carrivick et al. 2012) resulting in thermal habitat niches.

Several studies have further identified point source thermal habitat niches at the streambed interface as selection criterion by many species of fish in choosing spawning locations and their subsequent construction of redds (Hendricks and White 1988; Muhlfeld 2002; Baxter et al. 2003; Hannah et al. 2004). However, much uncertainty remains on whether these animals select the micro-scale thermal refugia or are more generally attracted to temperature modulated reach scale conditions. Differentiation between these scales becomes particularly relevant when evaluating anthropogenic impacts (such as water taking, mining, urbanization, etc.) on spawning habitats as both the spatial and temporal river extents and subsequent measures of mitigation may vary widely.

A contributing factor in defining thermal refugia and spawning site scales is in the dearth of studies measuring streambed temperatures at sufficient spatial resolution and precision, principally attributed to the logistics, time and resources required in undertaking such studies. Consequently, broad assumptions of spawning preferences based upon sparse thermal observations are common place (e.g., Hendricks and White 1988; Rieman and McIntyre 1996; Muhlfeld 2002).

The recent development of a high-resolution thermal survey network (HI-RES TMD, presented in Chapter 2) provides an opportunity to better characterize streambed temperatures at the sub-redd scale and correlate the findings to redd locations. Two watercourses in southeastern British Columbia, Canada were thermally mapped using the system over the summer low-flow period of 2014 and spatially correlated to both cutthroat trout (*oncorhynchus clarkii*) and bull trout (*salvelinus confluentus*) redds

surveyed between 2012 and 2014. Several different analyses were completed to determine spatial correlations and causality between redds and micro-scale thermal refugia within the study reaches.

3.2 Background

The total thermal energy flux (Q_n) per unit volume of streambed can by expressed by (modified from Hannah et al. 2004):

$$Q_n = \pm Q^* \pm Q_h \pm Q_e \pm Q_b \pm Q_f \pm Q_a \pm Q_O$$

where Q^* is the net radiation, Q_h is the sensible heat (i.e., annual radiation cycle, water column temperature gradients), Q_e is the latent heat (evaporation and condensation), Q_b is the bed conduction, Q_f is friction generated between the bed and banks, Q_a is the heat and advection from submerged flow and Q_O are other heat sources/sinks from such things as river confluencing. The relative contribution of each of these parameters to the magnitude of thermal energy varies at different special scales.

Frictional energy flux (Q_f) results from resistance to flow along the wetted perimeter of the channel which increases with increasing channel velocities. Therefore, Q_f increases per unit volume of water in regions of increasing channel slope or temporally when experiencing floods. In the case of the current study, observations are made and correlated to spawning sites which occur at low flow conditions where energy grade line slopes are small (Fraley and Shepard 1989). Therefore, spatial velocity gradients magnitude and therefore Q_f is assumed to be negligible and unlikely to vary at the sub-meter scale under low-flow conditions (Webb and Zhang 1997).

Sensible (Q_h) and latent heat (Q_e) have significant temporal variations, but are relatively spatially constant at the river reach scale (Hannah et al. 2008; Carrivick et al. 2012; Kim et al. 2014). Net radiation (Q^*) can spatially vary along a reach depending upon the distribution of cloud cover which can be further modified by riparian cover shading along the stream banks (Beschta 1997; Johnson 2004) . Depending on the alignment of the watercourse and the positioning, density and extent of riparian cover, net radiation can have diurnal spatial variability resulting in transient spatial cold spots during spring and fall spawning seasons making the spatial variability of radiation energy flux difficult to quantify at both the reach and micro scale (Hannah et al. 2008). Overhanging riparian cover also provides visual protection to fish from predators, and shaded areas have previously been identified as desirable locations for redd construction (Knapp and Preisler 1999; Zimmer and Power 2006).

Spatial variability of bed conduction (Q_b) is dependent upon the minerology and heterogeneity of the stream bed material. For uniform river bed material systems (i.e., bedrock channels) this variance is negligible, however for alluvial systems, variability in thermal capacity can increase with increasing heterogeneity of bed material minerology between particles (Côté and Konrad 2005). Bed material sorting can also influence streambed conduction as coarse grained materials (such as gravels and cobbles) will

have lower thermal capacity relative to finer-grained material of equal porosity (Barry-Macaulay et al. 2015). The thermal capacity can also be modified at the grain-scale by the female spawning salmonids as they sweep fines from the inter-spatial voids of the nests during redd construction (Burner 1951), which could indicate that the desired areas for spawning have lower thermal capacity than the surrounding channel bed. The process of clearing fine-grained material has also been shown to decrease embryo mortality (Lisle and Lewis 1992) and increase hyporheic flow through around embryos (Vaux 1967; Marchildon 2009).

Thermal capacity of granular material can further increase with increasing saturation of the material, consequently, areas of partially exposed streambed (i.e., low flow sections such as riffle crests, point bars, transverse bars or locations along the banks) would require more energy to increase their temperature (Barry-Macaulay et al. 2015). Conversely, as flow depth increases providing more insulation to the channel bed, thermal variations from atmospheric energy (i.e., convection) decrease.

Annual fluctuations in groundwater temperatures are significantly smaller than those of surface water bodies exposed to atmospheric conditions (5-10°C versus 25-30°C respectively, Kim et al. (2014)). This results in particularly detectable thermal gradients (Q_a) between upwelling groundwater and surface water bodies during summer and winter low-flow periods where groundwater is commonly colder or warmer respectively, relative to the surface water temperatures. Spatial variability in thermal conditions arising from groundwater upwelling and hyporheic flow into rivers has been well documented at the reach and morphometric scale (Tonina and Buffington 2009). However, alluvial gravel- and cobble-bed rivers (such as those studied here), have complex depositional streambeds, which can result in large sub-metre variability of hydraulic conductivities in a three-dimensional framework (Tonina and Buffington 2009; Käser et al. 2013; Trauth et al. 2015). Temperature measurements have often been made within redds supporting the conjecture that spawning site selection locations gravitate towards upwelling locations at the micro fluviatile-scale (Baxter et al. 2003; Cardenas 2015; Trauth et al. 2015). However, in many studies, temperatures were not measured at comparable resolution beyond the limits of redds to quantify the spatial correlations with redd selection locations and thermal gradients.

Many other abiotic metrics have been attributed to the specific site selection preferences of salmonids such as: bed material grain size distribution (Kondolf and Wolman 1993; Baxter and McPhail 1997; Muhlfeld 2002; Mull and Wilzbach 2007), hydraulic properties such as Reynolds Number, flow depth, flow velocity and turbulence (Lounder 2011; Marchildon et al. 2011; Marchildon et al. 2012) and, water quality (Hansen 1975; Ringler and Hall 1975; Geist 2000; Bickel and Closs 2008). However, no single metric is deterministic in characterizing the selection locations by salmonids although several metrics

suggest a selection bias towards areas with lower thermal capacities and therefore cooler streambed temperatures are preferable.

3.3 Methods

3.3.1 Site Selection

Ram Creek and Lizard Creek, located along the western slope of the Rocky Mountains in southeastern British Columbia (BC) were selected as study sites. Selection criteria were predominantly based upon watercourses where significant historical salmonid spawning (in this case bull trout and cutthroat trout) was known to occur, as identified by experienced fisheries biologist. Bull trout commonly spawn in late summer and early fall (Kitano et al. 1994; Rieman and McIntyre 1996) when thermal gradients between surface water and groundwater are commonly the highest (groundwater is colder relative to the surface water conditions at this time of the year). Bull trout have been previously observed to spatially correlate with colder spatial zoning (White et al. 1987; Hendricks and White 1988; Muhlfeld 2002; Hannah et al. 2004). Conversely, cutthroat trout spawn in the late spring/early summer, which, in southeastern BC, coincides with the spring freshet (Rieman and McIntyre 1993; Muhlfeld 2002). During this period, surface waters temperatures decrease from the thermal flux of melt waters. As groundwater temperatures remain relatively constant throughout the year (Kim et al. 2014), groundwater temperatures would be typified by warmer temperature zones, relative to the surface water, to the spawning animals and for thermal surveys conducted as soon as logistically possible the spring snow melt (i.e., freshet).

Each creek drains predominantly forested catchments with minor anthropogenic impacts (i.e., logging roads). Geomorphic surveys were completed in July 2014 to characterize morphological features using a first order differential GPS (±1 cm accuracy). Furthermore, sediment sampling was completed in October 2014 to characterise the representative grain size distribution of the streambed. Both surveys and sediment sampling were completed using the methods outlined by Annable (1996). Pools were classified using the methodology defined by Lisle (1987) and riffle crests and bottoms were field identified. Runs were later identified as areas not classified as pools or riffles (Montgomery and Buffington 1997). Table 3-1 lists the fluvial characteristics of both study sites.

Table 3-1: General morphological conditions of Ram Creek and Lizard Creek

Characteristic	Units	Ram Creek	Lizard Creek
Dominant spawning species		bull trout	cutthroat trout
Average bankfull width	m	17.5	9.3
Average bankfull depth	m	1.0	0.6
Average flow depth (during data collection)	m	0.21	0.18
Elevation (downsteam and upstream)	m	1086.67–1091.24	1007.76–1011.06
Main channel length	m	518	380.18
Average slope	%	0.9	0.9
Sinuosity	-	1.4	1.2
Average D_{10}, D_{50}, D_{90}	mm	10, 110, 160	-
General bed material classification	-	Cobble	Gravel
Rosgen Classification (1994)	-	B3c	B4c
Montgomery and Buffington Classification (1997)	-	Plane-bed	Plane-bed

Redd surveys were completed with the assistance of experienced fisheries biologist during the fall of 2012, 2013 and, 2014 and spring of 2013 and 2014. Redds were identified within the streambed as oval patterns of clean, well sorted bed material, with a depression at the upstream extent of the oval (Burner 1951). Figure 3-1 illustrates the spawning technique which is used by both species and an example of the resulting bed material. The limits of every redd were delineated with an average of six survey points using a first-order differential GPS (±1 cm accuracy). Cutthroat redds averaged 1.7 m in length by 0.8 m in width whereas bull trout redds averaged 2 m and 1 m respectively. A total of 15 cutthroat trout and zero bull trout redds were identified on Lizard Creek and 101 bull trout and two cutthroat redds were identified on Ram Creek between 2012 and 2014. On Ram Creek, some of the bull trout redds had multiple pits identified, however, the limits of individual redds could not be determined as several females super positioned spawning on the same locations. At these locations, the limits of the multiple pits were delineated as single polygons. Therefore, a total of 120 individual bull trout redd pits were identified. Spawning densities were calculated using the number of pits identified as this was more representative of the localized spawning activities. Based upon these survey results, for the purposes of this study, Lizard Creek was classified as cutthroat trout dominated and Ram Creek as bull trout dominated watercourse. A summary of the redd surveys is included in Appendix B which stratifies observations by morphological features associated with redd spawning.

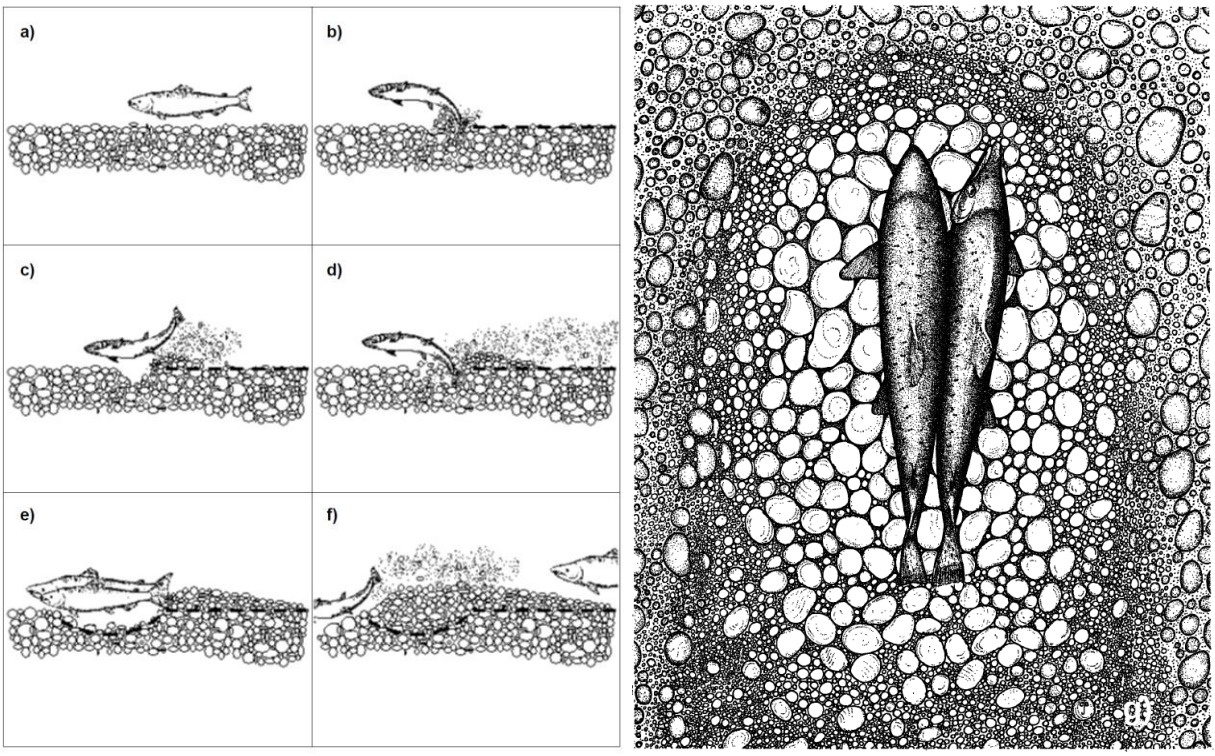

Figure 3-1: Illustration of the salmonid spawning technique within a river setting. a) Pre-spawning stage; b) cutting; c) displacement of streambed material; d) transport of fine-grained sediment downstream; e) oviposition; f) covering of fertilized ova and subsequent upstream pit excavation (Marchildon 2009). g) Resulting well sorted bed material within the redd (Burner 1951).

For the species investigated in this study, previous studies have identified that the downstream limits of pools and glides are the morphological units where spawning has been preferentially observed whereas riffles were found to be less desirable locations (Geist and Dauble 1998; Hanrahan 2007). Here, Ram Creek observed 4% of the surveyed redds on riffles despite the riffles covering 29% of the reach and no redds were observed on the riffles of Lizard Creek, which cover 25% of the reach. The distribution of redds between pools and runs along both creeks were similar with 41% and 46% of the redds on pools for Ram and Lizard Creeks respectively and 55% and 53% on runs respectively. The location of redds within the pools was scattered and not concentrated to the downstream extents of each feature, as had been previously documented (Geist and Dauble 1998; Hanrahan 2007).

Between the fall of 2013 and spring of 2014, Ram Creek experienced an average 20 m lateral shift along an approximate 100 m sub-reach as a result of a large magnitude low frequency flood event. These types of channel shifts are common during such events and can be further magnified by steep gradient systems

and hydraulic interactions proximal to confluences (Leopold et al. 2012), which are consistent with the study site conditions. Therefore, between the 2013 and 2014 spawning seasons, the river abandoned 12% of the bull trout redds within the wetted perimeter limits of the bankfull channel - which had been infilled with coarse alluvial material. No cutthroat trout redds were abandoned. As the thermal investigations were completed in 2014 (post flood), the analyses completed does not consider redds in the abandoned channel section.

In order to characterize the abundance and overall repeatability of spawning sites at each site, redds were assigned three different classifications: annual density (ρ_A), cumulative density (ρ) and, repeatability in spawning location (ρ_R) which were determined as follows:

- ρ_A of redd *i* is equal the total number of redds within a 10 m radius surveyed within the same sampling year as redd *i*,
- ρ is the total number of redds within a 10 m radius of redd *i*, regardless of the year of observation.
- ρ_R is number of years of observation of all the redds within a 10 m radius that differ from redd *i*, As an example, the maximum ρ_R possible for the Ram Creek study reach would be 2. This would occur if redds from 2012, 2013 and 2014 were within 10 m of each other.

Resulting values of ρ_A, ρ, and ρ_R are presented in classed post maps in Figure 3-2. Annual and cumulative densities at Ram Creek are much higher than Lizard Creek, as there was significantly more spawning at Ram Creek. Within the Ram Creek study area, there are isolated regions that have high ρ_A, ρ, and ρ_R values.

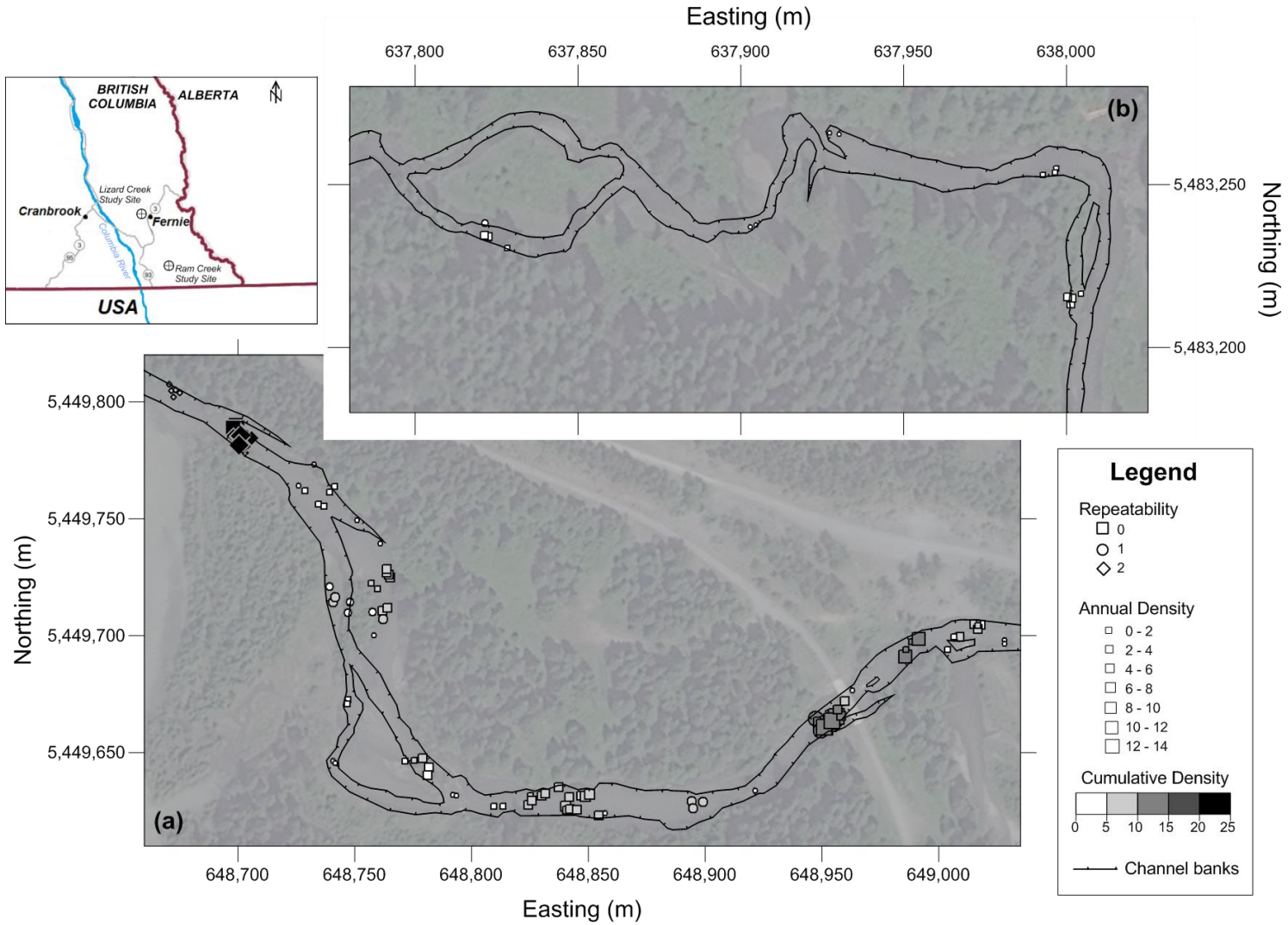

Figure 3-2: Annual density, cumulative density and repeatability of redd surveys between 2012 and 2014 of a) Ram Creek and b) Lizard Creek study reaches.

3.3.2 Thermal Data Collection

Streambed temperature measurements were collected (n > 80,000) using the non-invasive High-Resolution Conductivity and Temperature array (HI-RES TMD) system (Chapter 2) along the two study reaches. The system was developed to measure high resolution streambed temperatures while overcoming several other common constraints of field investigations (such as limited spatial extents and/or time consuming procedures). The array features 32 conductivity and temperature probes, spaced 0.3 m apart in a planometric grid pattern (3 m^2). The entire apparatus is constructed from rugged aluminum and is approximately 1.2 m wide and 2.5 m long. Total station prism mounts are integrated into the four corners of the frame to geospatially locate the apparatus using a total station theodolite or a first-order differential GPS. In this case a Trimble Robotic S6 total station (±2 mm, Trimble Navigation Ltd. (2013)) was used. By georeferencing the four corners of the frame, georeferenced coordinates of each discrete sampling probe could subsequently be calculated.

HI-RES TMD records one flow depth measurement for every 32 probe measurement positions (subsequently referred to as a cage). Flow depth (m) is recorded from a 2 cm graded staff gauge located on one of the upstream legs of the device. Water surface elevations are therefore assumed constant within each cage measurement (one depth measurement per 3 m^2) which remains at a higher survey resolution relative to recommended methodologies for bathymetry surveys (Levec and Skinner 2004). Using the above assumption, flow depth for each probe was estimated by linearly interpolating between staff gauge measurements of adjacent cages.

Due to the design of the HI-RES TMD system, the maximum flow depth able to be investigated was 0.75 m. Deeper flow depths would have compromised the electronics of the equipment. Additional restrictions occurred where large protruding boulders, woody debris or overhanging vegetation prevented the placement of the sampling equipment. Obstacles were noted, circumvented and sampling was performed as close as logistically possible to each protrusion. Obstacles accounted for approximately 10% and 6% of the channel area of Ram Creek and Lizard Creek respectively.

Streambed temperature data were collected at Ram Creek between late July and early September 2014, and at Lizard Creek during the month of September, 2014. It is expected that temperature gradients between upwelling groundwater and surface water (as influenced by atmospheric conditions) had the highest contrast during these periods. In both cases, data collection was performed during the day, between 8:00 hrs and 18:00 hrs. A tacit assumption in deploying the HI-RES TMD system is in the measurement position at the streambed interface. Other researchers have found that detecting groundwater emergence was achievable when temperature measurements were acquired at depths

between 10 cm–15 cm into the stream bed material to dissipate boundary layer mixing (Muhlfeld 2002; Conant 2004; Kim et al. 2014). Using subsurface temperature measurements removes the majority of the diurnal fluctuations associated with the streambed temperatures measurements, which also allows the lag time between measurements to be higher. Using the HI-RES TMD system, 32 measurements are instantaneously acquired over 3 m^2 (which is similar in area to the redd scale) resulting in a method that can detect changes in stream bed temperatures, relative to each other, also removing any sampling lag time between adjacent measurements, with significantly reduced effort. Detectable thermal gradients are muted, relative to measured temperatures 10 cm–15cm within the subgrade, however, they are considered more representative to the temperatures experienced by the salmonids during the spawning selection process at the streambed interface.

The measured streambed dataset averaged a spatial resolution of 0.09 m^2 covering approximately 5200 m^2 on Ram Creek and 2300 m^2 on Lizard Creek (Figure 3-3). Several other parameters such as flow depth, air temperature and solar radiation were collected during the sampling periods in conjunction with the on-board measurements system. Table 3-2 summarizes the data collected along both study sites. Observations were removed for probes resting on bed material or other small obstructions above the water surface or in cases of inoperable probes as per the methods outlined in Chapter 2.

Table 3-2: Summary of data collected on Ram Creek and Lizard Creek

Data Parameter	Ram Creek	Lizard Creek
Total number of cages within the study reach	1,841	939
Total number of streambed temperature samples	58,912	30,048
Total number of streambed temperature samples post error removal	58,404	29,949
Number of field days	20	12
Average number of measurements per day	2,920	2,496
Length of river over which temperature samples were collected (m)	720	500
Area of river over which temperature samples were collected (m^2)	5,200	2,300

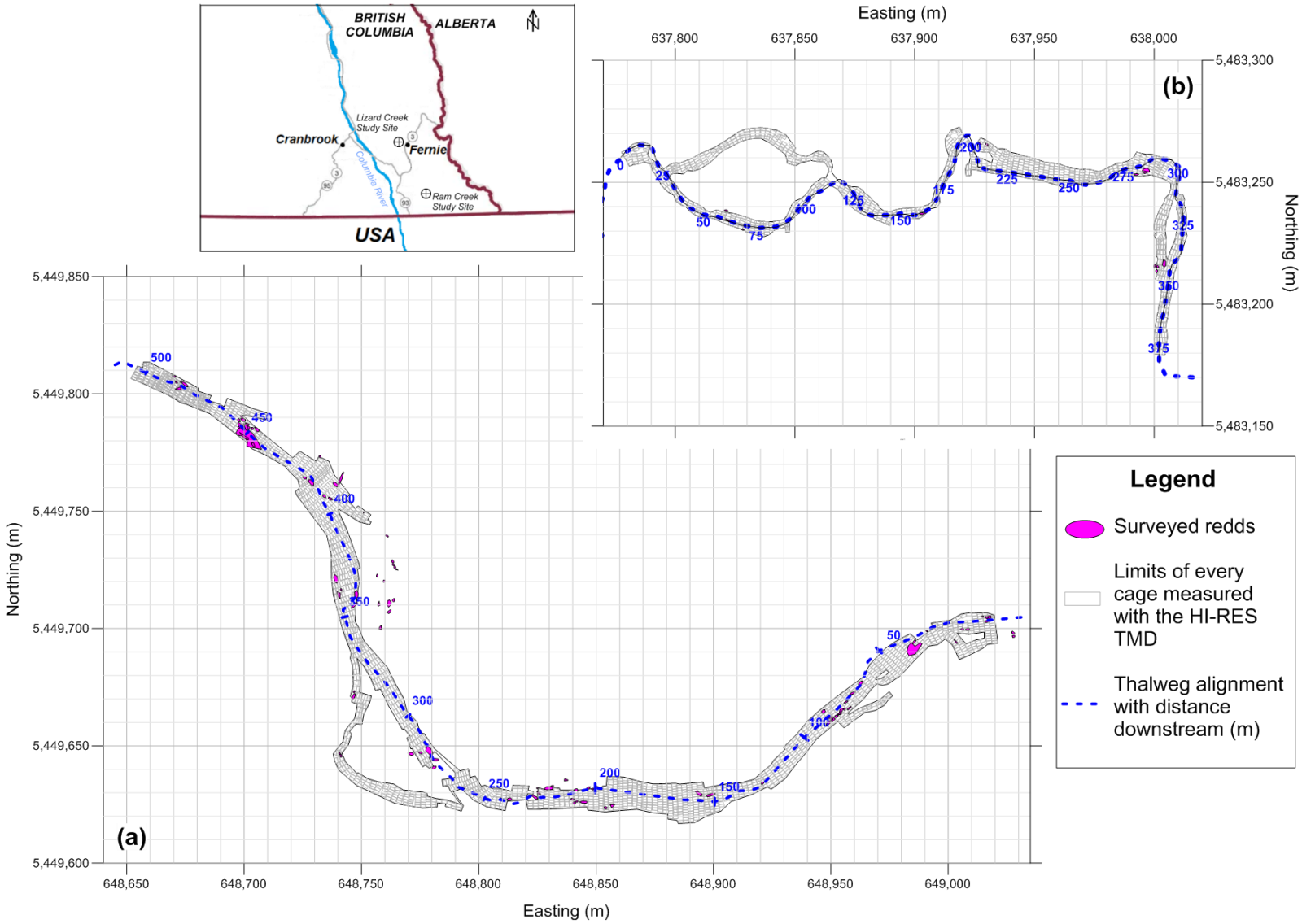

Figure 3-3: Extents of thermal study reaches with surveyed redd locations for a) Ram Creek and b) Lizzard Creek.

3.3.3 Data Processing

As the HI-RES TMD system can be used over a large area within a single day and amongst several days of field surveys, diurnal fluctuations within the sampling parameters must be removed to spatially compare the data. In order to incorporate the irregularity of the variance, a standard score normalization was employed in conjunction with a temporal moving window. A standard score represents the number of standard deviations of each value from the average of the sample which can also be presented as the probability of any temperature within the moving window to be less than that of the sample. As sample sizes (n) within the moving windows were greater than 30, a Gaussian distribution standard score was employed instead of a t-Distribution (Walpole et al. 1993). This method was able to provide the necessary fluidity of the data, and identify values that varied from the mean of the moving window.

The normalization values of standard score (Z_{ijk}) and probability (p_{ijk}) were defined as (Walpole et al. 1993; Mohamad and Usman 2013):

$$Z_{ijk} = \frac{T_{ijk} - \mu_{MW}}{\sigma_{MW}} \qquad \text{where } -\infty \leq Z_{ijk} \leq \infty$$

$$p_{ijk} = \frac{1}{\sigma_{MW}\sqrt{2\pi}} \cdot e^{\frac{-(T_{ijk}-\mu_{MW})^2}{2\sigma^2}} \qquad \text{where } 0 < p_{ijk} < 1$$

respectively, where

$$\mu_{MW} = \frac{1}{5}\sum_{\gamma=k-2}^{k+2}\frac{1}{m}\sum_{\beta=1}^{m}\frac{1}{n}\sum_{\alpha=1}^{n} T_{\alpha\beta\gamma} \ \ (gemetric\ mean\ of\ the\ Moving\ Window\ (MW))$$

$$\sigma_{MW} = \sqrt{\sum_{\gamma=k-2}^{k+2}\sum_{\beta=1}^{m}\sum_{\alpha=1}^{n}\left(T_{\alpha\beta\gamma} - \mu_{MW}\right)^2} \ \ (standard\ deviation\ of\ the\ MW)$$

and T_{ijk} is the indexed temperature measurement for measurement i, of cage j and cross section k (which is comprised of m cages where each cage has n measurements). Details of the normalization of the data can be found in Chapter 2.

Based on preliminary screening of the data a series of statistical and autocorrelation methods were selected to analyze the data. The analytical methods used are presented below.

3.3.4 Statistical and Spatial Analysis Methods

3.3.4.1 Bonferroni t-Test

The Bonferroni t-Test uses statistical hypothesis testing to determine the significance at which the means of two populations are the same. For this test, the null hypothesis (H_0) assumes that the means of the two populations (e.g., all the temperature data from two reaches, two features, two redds, a feature and a redd, etc.) are equal, with the alternative hypothesis (H_1) assuming that they are not equal (with an unknown value) as defined by (Walpole et al. 1993):

$$H_O: \mu_1 - \mu_2 = 0$$

$$H_1: \mu_1 \neq \mu_2$$

An observed t-value (t_{obs}) is calculated for the two populations and is compared to the critical value $\left(t_{\frac{\alpha}{2}}\right)$ representing the maximum acceptable error in result. If the observed t-value is less than the critical value, the null hypothesis is accepted and the means are assumed equal to a predetermined significance (α) (Walpole et al. 1993). The test assumes that the populations are normally distributed. The parameters are calculated as follows (Walpole et al., 1993):

$$t_{obs} = \frac{|\overline{x}_1 - \overline{x}_2|}{v\sqrt{\frac{s_1^2}{n_1} + \frac{s_2^2}{n_2}}}$$

$$v = \frac{\left[\frac{s_1^2}{n_1} + \frac{s_2^2}{n_2}\right]^2}{\left[\left(\frac{s_1^2}{n_1}\right)^2 \frac{1}{n_1 - 1}\right] + \left[\left(\frac{s_2^2}{n_2}\right)^2 \frac{1}{n_2 - 1}\right]}$$

Where $\overline{x}_i$ of the sample mean, s_i^2 is the sample variance, n_i is the sample size. The variance coeifficent (v) is the Smith Sattherwaite Approximation, which was used because it was unknown if the population variance were equal (Walpole et al. 1993). Unless specified otherwise, a 5% significance level was used for the analysis. The t-Test analysis allows for broad scale comparison of the datasets where an exact spatial representation of the data would not further contribute to the analysis. This test was used to compare the thermal distributions between the study reaches, morphological features, and between the redds and morphological features. Specific uses of the t-Tests are identified within the Results.

3.3.4.2 F-Test

The F-Test uses statistical hypothesis testing to determine the significance at which the variance of two populations are the same. For this test, the null hypothesis (H_0) assumes that the means of the two

populations have equal variance, while the alternative hypothesis (H_1) assumes that they are not equal (with an unknown value) as defined by (Walpole et al. 1993):

$$H_O: \frac{\sigma_1^2}{\sigma_1^2} = 1$$

$$H_1: \frac{\sigma_1^2}{\sigma_1^2} > 1$$

An observed f-value (f_{obs}) is calculated for two populations, similar to the example described for the t-Test analysis, and is compared to the critical value $\left(f_{(\alpha,df1,df2)}\right)$ representing the maximum acceptable error in result. The null hypothesis is accepted if the observed f-value is less than the critical, and the variance are assumed equal at a significance of α (Walpole et al. 1993). The parameters are calculated as follows (Walpole et al. 1993):

$$f_{obs} = \frac{s_1^2}{s_2^2}$$

The critical f-statistic ($f_{(\alpha,df1,df2)}$) is determined for a significance of α, where the degrees of freedom (df_1 and df_2) are equal to the one less than the sample sizes (n_1 and n_2). Similarly to the Bonferroni t-Test, a significance of 5% was used for the analysis, unless specified otherwise. The F-Test analysis allows for broad scale comparison of the datasets where an exact spatial representation of the data would not contribute further to the analysis. This test was used to compare the thermal distributions between the study reaches, morphological features, and between the redds and morphological features. Specific uses of the F-Tests are identified within Section 3.4.

3.3.4.3 Least Significant Difference (LSD) Test

The Least Significant Difference (LSD) is a modification of the Bonferroni t-Test which compares the means of multiple samples to determine which are significantly similar (at a significance of α). In this study it compares the thermal distributions of morphological features to those of the redds. The LSD is product of the standard error of all the sample and critical statistic as defined by (Walpole et al. 1993):

$$LSD = (s.e.)\left(t_{\frac{a}{2},\bar{n}}\right)$$

where

$$s.e. = \sqrt{\frac{2\ MS(Res)}{\overline{n}}}$$

The mean squared residual error of the samples (*MS(Res)*) is determined from a multiple parameter analysis of variance (ANOVA). If the difference between the means of two populations is greater than the LSD, the samples are considered to be significantly different, and if the difference is less than the LSD the inverse is assumed. As the probability of making a single incorrect rejection increases with the number of samples (i.e., Type II hypothesis testing error) included in the analysis, significance levels were tested specifically to reduce this error.

3.3.4.4 Spatial Autocorrelation (SAC) Analysis

Spatial autocorrelation analysis (commonly referred to as hotspot analysis) is used to quantify correlations between spatially dependent data (Lee and Wong 2001). These methods are commonly used for viral outbreak monitoring (Haining 2003; Getis and Ord 2010) contaminant fate delineation (Albert et al. 2000; de la Torre et al. 2012) and radial heat analysis (Getis and Ord 2010; Golden et al. 2015).

A local, G_i^* (referred to as the Getis-Ord, G_i^* analysis) analysis was used to quantify the correlation of the standardized temperature data (Z_{ijk}) to the surrounding measurements as defined by (Getis and Ord 2010):

$$G_i^*(d) = \frac{\sum_j w_{ij}(d) \cdot x_j}{\sum_j x_j}$$

Where $w_{ij}(d)$ is binary matrix indicating true if x_j within a distance of d from x_i. A large positive value of G_i^* represents a strong correlation of hot temperature measurements within a radius of d of the measurement. Specifically, this would mean that the measurement at location i is hot (relative to the entire dataset) as well as the measurements within radius d. A large negative value of G_i^* would represent a strong correlation of cold temperature measurements. A G_i^* value can be calculated for every measurement obtained with HI-RES TMD grid limit (3 m^2), quantifying each temperature measurement to its surrounding measurements. This analysis was completed using the standardized temperature (Z_{ijk}) data, which removes the temporal variations of the data creating a dataset that was only spatially dependant (not temporally).

G_i^* can also be standardized to a Gaussian distribution score, which can then be used to identify measurements which have statistically significant correlations (Getis and Ord 2010) and are not within the normal distribution of the parameters being investigated as defined by:

$$Z_{Gi} = \frac{G_i^*(d) - E[G_i^*(d)]}{\sqrt{Var\left[G_i^*(d)\right]}}$$

Where

$$E[G_i^*(d)] = \frac{\sum_j w_{ij}(d) \cdot x_j}{n}$$

$$Var[G_i^*(d)] = \sqrt{\frac{\sum_j {x_j}^2}{n} - E\left[G_i^*(d)\right]}$$

The G_i^* method was preferable to other SAC analysis methods, such as the Geary, Moran *I*, or general *G* statistic methods (Lee and Wong 2001), as these other SAC methods provide a boarder scale correlation and the G_i^* provides a result that is relative to an exact location (Lee and Wong 2001; Getis and Ord 2010). It was also desirable to maintain the data resolution for comparison purposes between temperature hotspots and redds, therefore it was necessary to use a SAC analysis that was able to accommodate this.

Here the G_i^* method was used to define correlations of standardized temperature measurements and delineate the hottest and coldest regions within the both the Ram and Lizard Creek study reaches. This provided a foundation to spatially compare the locations of redds to the hot and cold spots. Due to the different species encountered at the two sites, it was expected that redds with the highest ρ_A, ρ, and ρ_R would also have the strongest correlation to the cold spots at Ram Creek as the temperature gradients were the highest. Redds at Lizard Creek were not expected to be correlated to cold spots or hot spots (henceforth referred to as significant spots) as all observed redds were associated with spring spawning cutthroat trout where surface water temperatures were similar to groundwater temperatures during the period of spawning.

The G_i^* analysis was completed using the Spatial Analysis Toolset within ArcGIS 10.2 (ESRI 2011). A series of calibrations were performed to determine the most representative *d* value for the G_i^* calculation. Initially the average length (2 m) and width (1 m) of redds were used to represent *d*; however, both these values proved to be too large as resulting significant spots represented more than 60% of the study reach. A *d* value of 0.5 m was then used as this is the smallest size to ensure that every point has a single neighbour (Lee and Wong 2001; Getis and Ord 2010; ESRI 2011). The G_i^* value was standardized (Z_{Gi*}) to allow for relative comparison to the normal distribution of the data.

Locations of each streambed temperature measurement were converted to representative areas using the Thiessen polygon transformation (ESRI 2011). The average area allocated to each measurement was

approximately 0.09 m^2. Each polygon retained the standardized temperature of the measurement it encompassed, and the associated Z_{Gi*}. All adjacent areas with $Z_{Gi*} \geq$ 95% significance levels (1.96), or $\leq$ 5% significance (-1.96), were amalgamated to form statistically significant spots.

3.3.4.5 Redd Proximity Metric

Redds positioned within significant spots were identified and quantified within ArcGIS. However, a super-positioning comparison disregards redds that were near significant spots, but not directly encompassed. Therefore, to quantify spatial correlations between significant spots and redds (super-positioned and proximal), a redd proximity metric (R_i) was defined. R_i is a weighted cumulative score for each redd representing standardized temperature and the surrounding significant spots in relation to the squared distance between significant spots and a given red defined by:

$$R_i = \sum_{n=1}^{k} \frac{\overline{Z_{ijk}}_n \cdot A_n}{{l_n}^2} \cdot w(50)_{ni}$$

Where $\overline{Z_{ijk}}_n$ is the average, standardize temperature of significant spot n of a total of k significant spots, A_n is the area of significant spot n, l_n is the separation distance between the centroids of the significant spot n and redd i, and $w(50)_{ni}$ is a binary matrix;1 if the distance between redd i and significant spot n is less than 50 m.

As l_n is a Euclidean distance (as opposed to the river thalweg path) a maximum separation distance (l_n) of 50 m was established (approximately two channel widths) to ensure that the limits of the channel were respected. R_i was calculated as a cumulative score of all the surrounding significant spots to create an unbiased representation of the entire thermal environment surrounding each redd, as opposed to just considering the hot or cold locations. Figure 3-4 illustrates the calculation method of R_i for each redd.

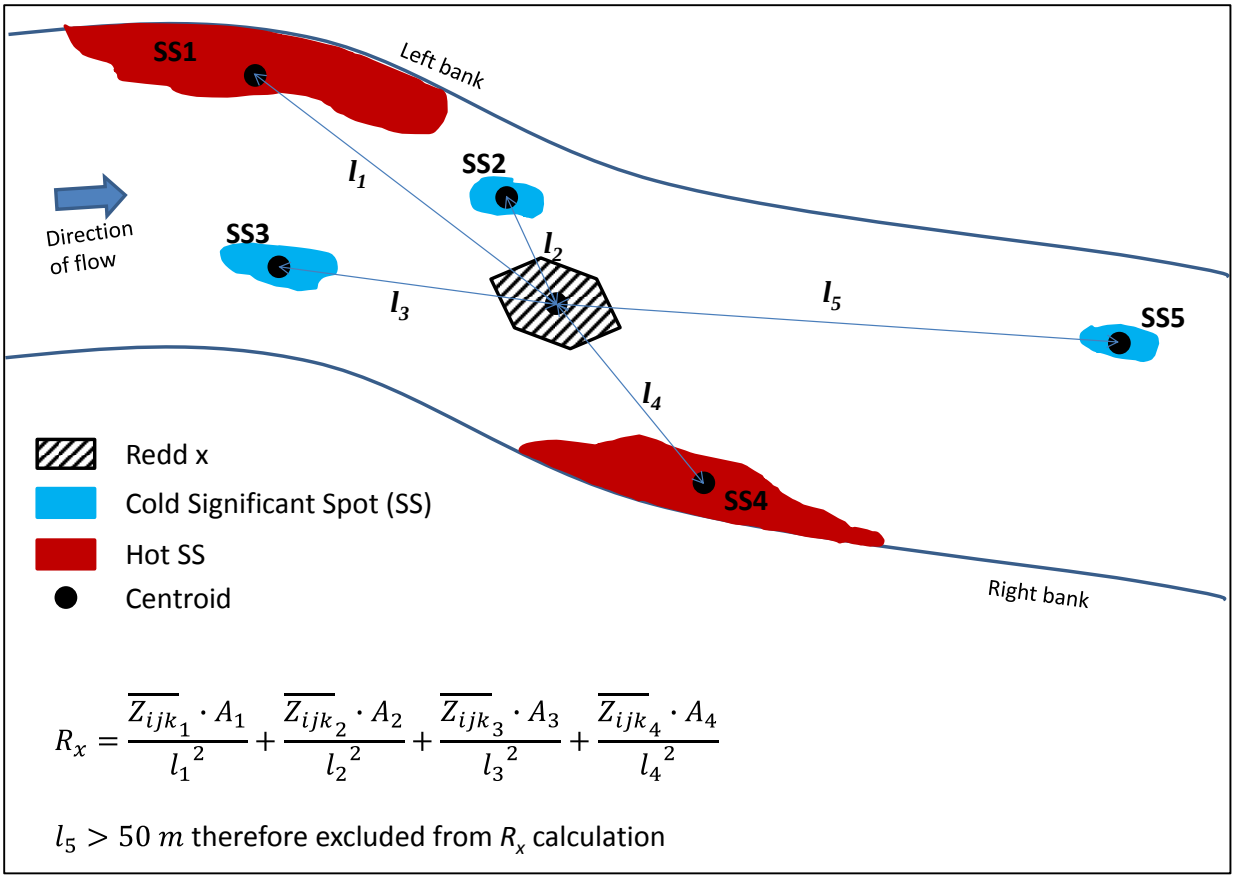

Figure 3-4: Schematic illustrating how the redd proximity metric (R_i) is calculated for a representative redd

To establish a relative significance, R_i values were calculated for every temperature measurement location for both study reaches, and a 95% confidence interval was determined for each reach. Therefore, if R_i for redd *i* was determined to exceed the upper limit of the confidence interval, the redd was statistically significantly correlated to hot spots and if R_i was less than the lower limit of the confidence interval, redd *i* was statistically significantly correlated to cold spots.

3.4 Results

3.4.1 Visual Analysis

For both study reaches, isotherms of the standardized temperatures were mapped using Surfer 13 (Golden Software, 2015) on a 0.5 m x 0.5 m (0.25 m^2) planometric grid to identify general spatial thermal variations (Figures 3-5 and 3-6). Given the average thermal sampling resolution (0.09 m^2), contours were generated using linear interpolation with triangulation.

The majority of both study areas had standard temperatures (Z_{ijk}) between -1 and 1; indicating that the temperatures are within one standard deviation of the temporal median sample temperature and therefore exhibited very small spatial variance across both study sites. While the majority of the streambed temperatures were approximately equal, there were visually identifiable clusters and delineations of hotter areas ($Z_{ijk} \geq 2$) and colder areas ($Z_{ijk} \leq -2$). Greater than 20 and 15 hotter areas were identified within the Ram Creek and Lizard Creek sites respectively, whereas fewer than 10 colder areas were identified at each site. Colder areas were commonly smaller in spatial extents relative to hotter zones. Along Ram Creek, warmer areas were concentrated primarily along the channel banks whereas warmer areas were more evenly distributed along Lizard Creek. The streambed at streambank margins would commonly be expected to exhibit increased thermal capacity as the areas typically maintain the shallowest flow depths and the finest sediment grain sizes (Wang et al. 2014). These areas would also experience thermal warming from the surrounding floodplain regions above the water table (Ochsner et al. 2001; Carrivick et al. 2012).

There were no visually obvious correlations (positive or negative) between hot and/or cold areas with the locations of redds at either study site. Redds were observed to super-position within the hot and cold areas on both study sites (Figures 3-5 and 3-6 (a), (b) and (c)) in addition to areas of average temperature. As the dataset presented here provides unprecedented resolution and extent of cover of streambed thermal measurements (inter- and intra-red), it is unlikely that spatial correlations at lesser scales and densities could be readily achieved and correlated based solely upon visual analysis techniques. Additional spatial analysis techniques need to be employed here to further investigate if redd placement correlates to either warmer and/or colder streambed temperatures and therefore potentially influence the discrete selection preferences of spawning salmonids.

Due to the limited normalized thermal variance, data classification and binning with statistical population comparisons will aid in identify similarities and differences between grouped temperature distributions. Temperature classes based upon morphological features will also be conducted as per the methods

outlined as there many thermal streambed patterns linked to morphological features (Bencala 2000; Tonina and Buffington 2007). Given the high resolution data set, spatially dependant variance techniques (such as SAC) will also be employed to evaluate the limits of each hot/cold spot and determine any correlations with the sizes, positions and distance between redds and hot/colds spots.

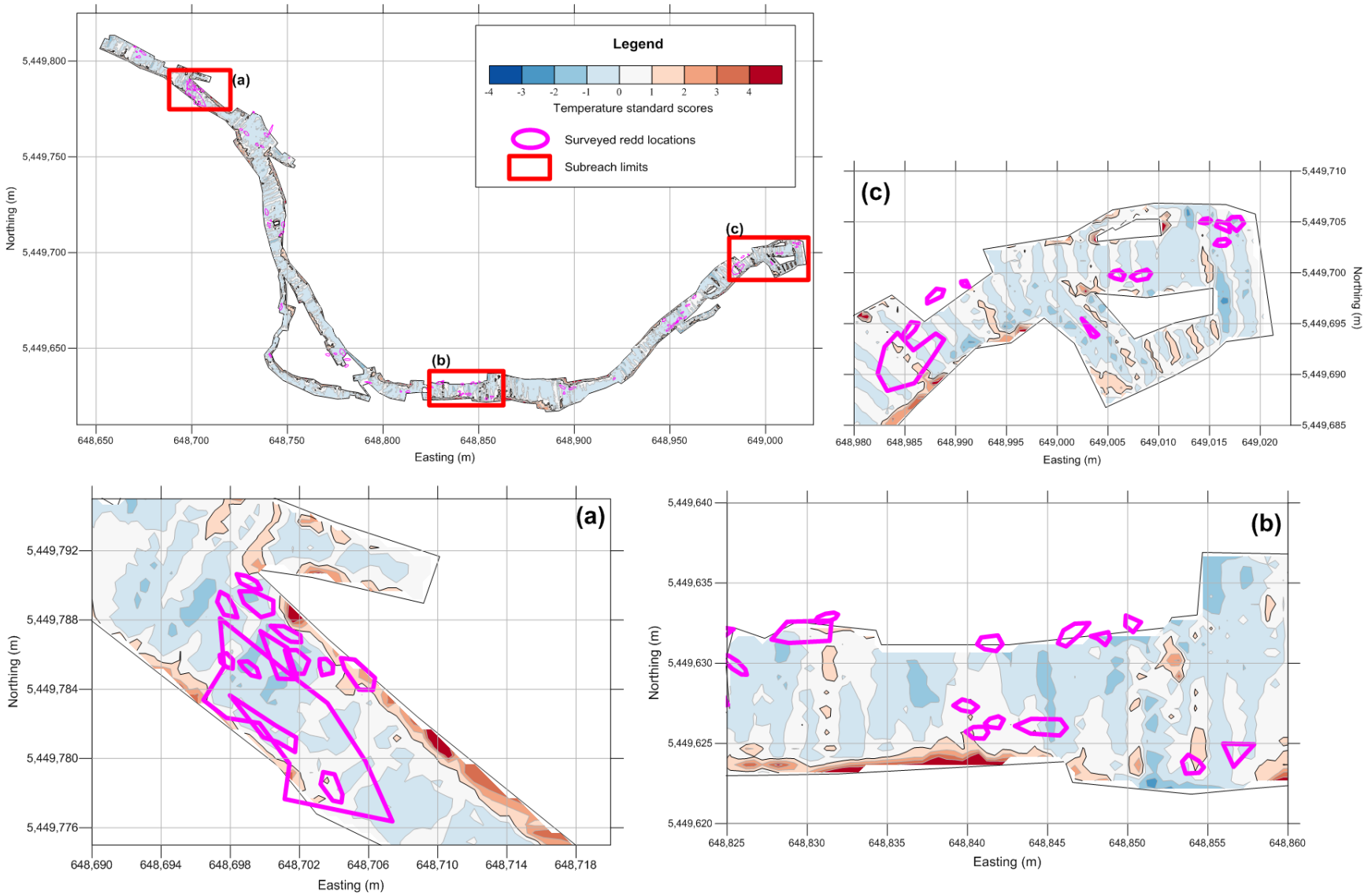

Figure 3-5: Isotherms of Ram Creek with magnified windows of interest

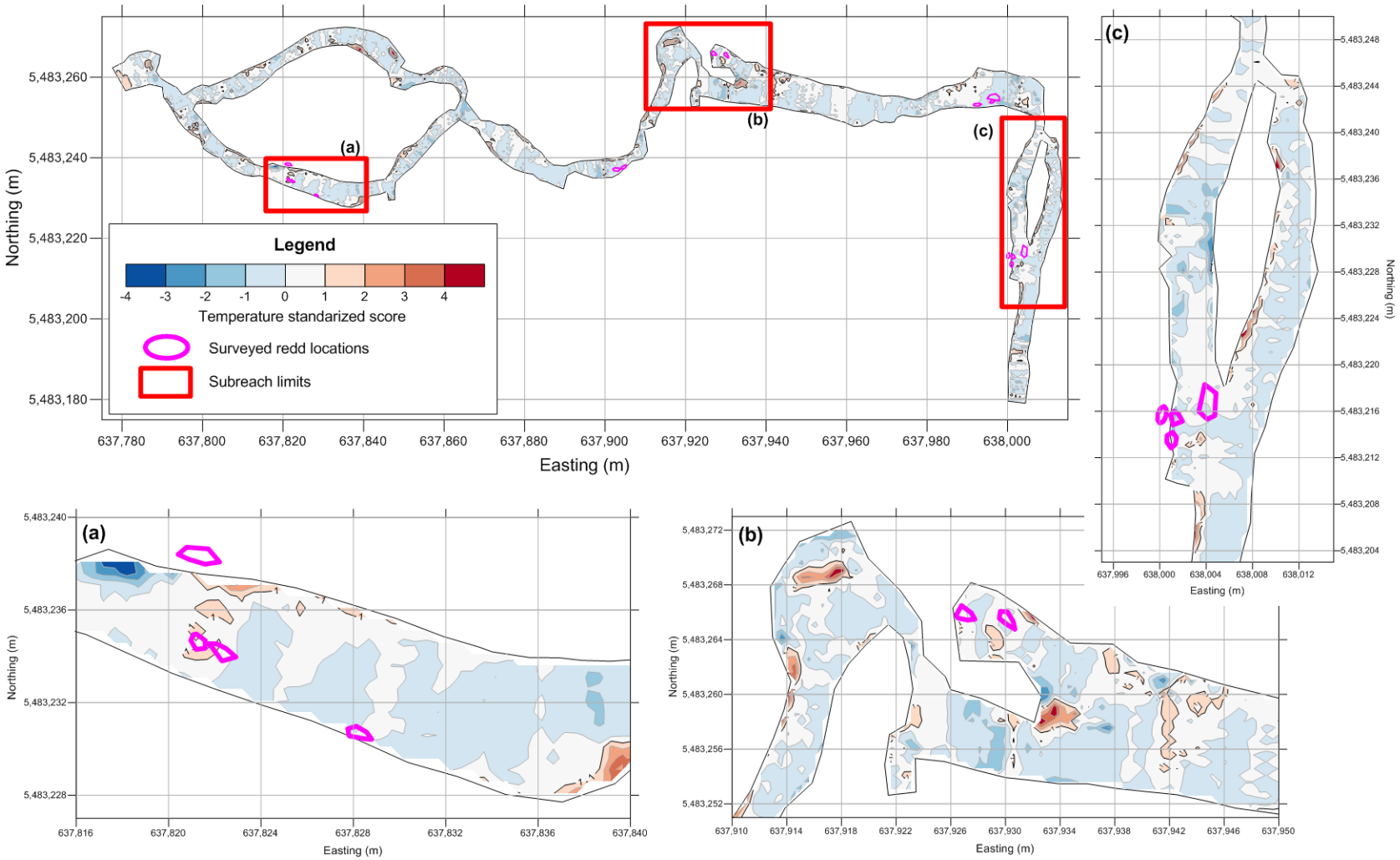

Figure 3-6: Isotherms of Lizard Creek with magnified windows of interest

3.4.2 Parameter comparison

The standardized temperatures (Z_{ijk}) were plotted against flow depth and solar radiation to determine if cross correlations existed as thermal energy flux of the streambed can be modulated by several additional parameters. Flow depth and exposure to solar radiation are two known parameters that contribute to the thermal energy flux, spatially vary and were measured during field investigations. Standardized temperatures were binned based on the corresponding flow depths and incoming radiation and geometric means and standard deviations of each class calculated and plotted (Figures 3-7 and 3-8).

Standardized temperature was correlated at both sites to flow depth through a fourth order polynomial equation. Standardized temperatures at flow depths less than 0.2 m were warmer and had a variance of 1.5 to 2 times greater than the rest of the observations. As the surface water insulates the streambed, flow depths less than 0.2 m, are likely more subject to atmospheric thermal variations and thusly dominated by the flux of the sensible and latent heat which is consistent with previous observations (Hannah et al. 2008; Buss et al. 2009). Therefore, thermal characteristics of the streambed within the low flow regions are dominated by non-spatially dependant parameters. Standardized temperatures at both study sites approached zero as flow depth increased to the maximum measurable limits (0.75 m).

It was observed that for flow depths less than approximately 0.175 m, Ram Creek has a warmer average standardized streambed temperature than Lizard Creek, but for flow depths greater than 0.175 m Lizard Creek has a warmer average temperature. Based on the established correlation between flow depth and standardized temperature, this would indicate that sensible heat effects (i.e., magnitude of atmospheric temperature) or latent heat effects (i.e., evaporation and condensation) were more dominant at Ram Creek than Lizard Creek. During the field investigation, the average atmospheric temperature during working hours was approximately 9°C higher during Ram Creek investigation versus Lizard Creek thermal measurements. This comparison provides further evidence that streambed temperatures within the low flow regions of the channel bed (such as riffle crests, stream bank margins, convex slopes of point bars and other depositional features) are dominantly controlled by non-spatially dependant energy parameters.

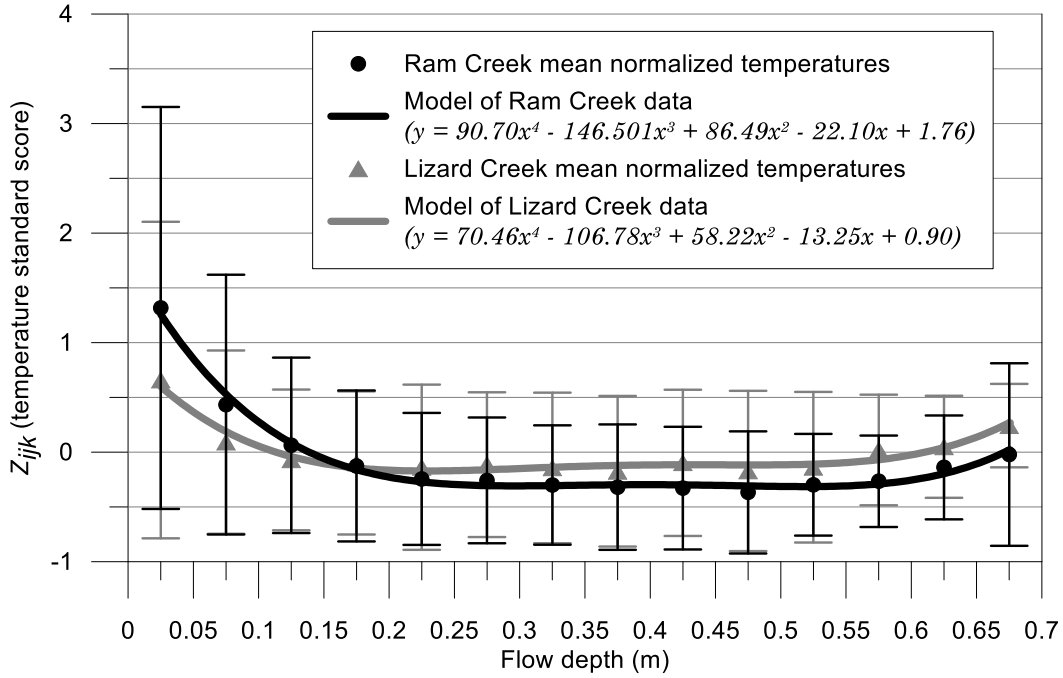

Figure 3-7: Relationship between standardized temperature and flow depth for both study sites. Error bars show the standard deviation.

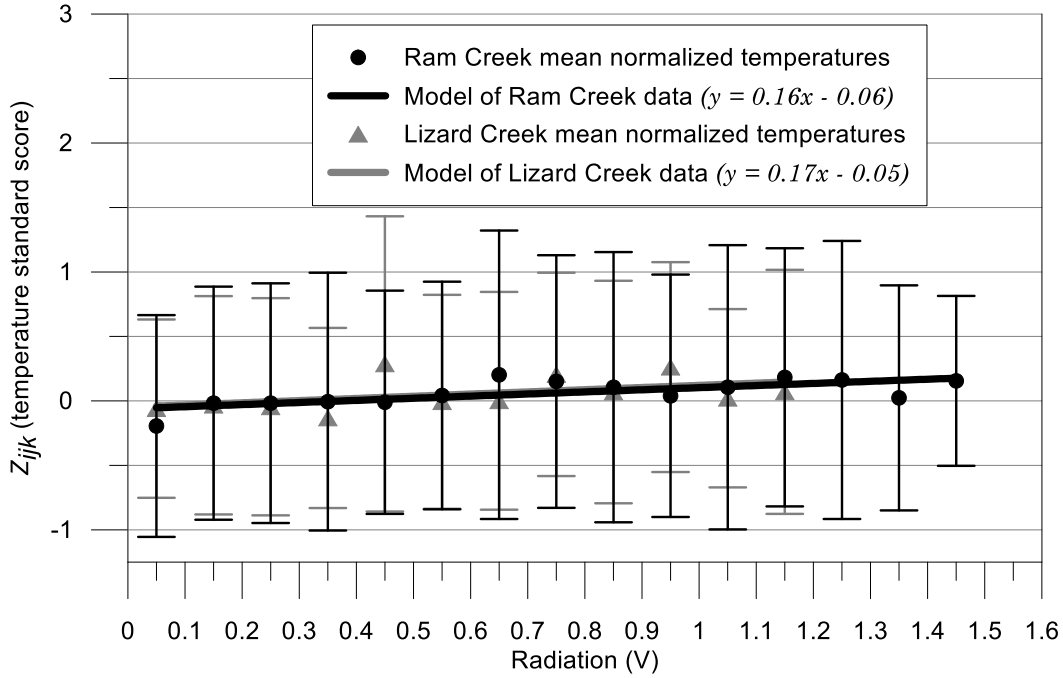

Figure 3-8: Relationship between standardized temperature and radiation for both study sites. Error bars show the standard deviation.

Standardized temperatures were correlated to solar radiation with linear relationships, however, the coefficients of the fitted equations were determined to be statistically insignificant, and the coefficients of determination (R^2) indicated that the fit represents less than half of the variance between the two parameters. It is possible that there was a time lag effect between incoming solar radiation and the streambed temperatures which was not able to be detectable or deconvoluted although it has been observed in several other studies (Edinger et al. 1968; Caissie 2006; Loheide and Gorelick 2006). Consequently, it is concluded here that the solar radiation (i.e., shading) observed at the time of measurement is not related to standardized streambed temperatures, however, the temporal lag effect of shading on streambed temperature may not have been correctly captured with the measurement apparatus.

Standardized temperature measurements exclusively obtained within redds were also assessed as a function of flow depth (Figure 3-9). At Ram Creek, standardized temperature correlated to flow depth as expressed by a fourth-order polynomial (Figure 3-9(a)). The trend mirrored the full dataset of Ram Creek (Figure 3-7) but was offset by an average of -0.75 identifying that redds are constructed in areas, on average, 0.75 standard temperature units colder than surrounding areas of similar flow depth. At Lizard Creek, the data were best fit to a second-order polynomial, however, statistical significance testing of the coefficients indicated that fit did not adequately represent the dataset. It was noted that the percentage of the total measurements within redds at Lizard Creek (0.6%) might have been too small to produce a representative sample, causing the lack of representativeness of the fit. Without a larger dataset to further examine the relationship, it was concluded that standardized temperatures within redds at Lizard Creek are not correlated to flow depth.

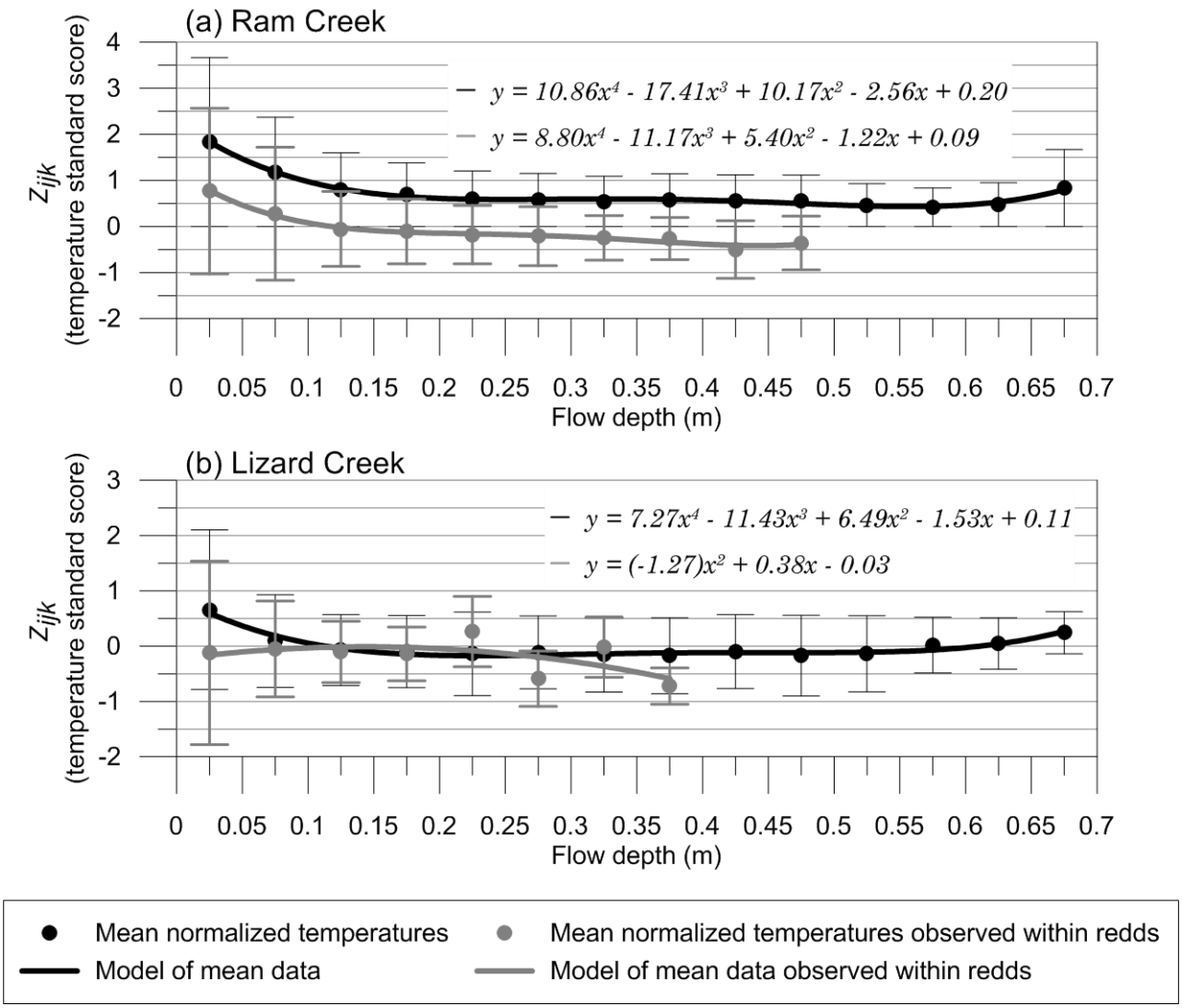

Figure 3-9: Relationship between standardized temperature and flow depth for both (a) Ram Creek and (b) Lizard Creek

3.4.3 Morphological Feature Statistical Population Comparison

Statistical population comparison analysis was completed to compare the thermal distributions of Ram Creek and Lizard Creek by morphological features. Establishing the similarities and differences between the reaches created a baseline for comparisons between the two study sites. This approach is also defendable based upon previous research where the animals were observed to commonly spawn on the lee end of pools and/or glides versus riffles (Geist and Dauble 1998; Hanrahan 2007). Morphologic feature stratification may deconvolute some of the spawning observations as there may be metrics external to this research that are playing a role in the site selection process that could be better stratified based upon morphological units (Imhol et al. 1996) .

Histograms of standardized temperature class were generated for each study reach (Figure 3-10). T-Test and F-Test analyses were completed for the two datasets identifying that the two reaches are considered to be statistically the same (mean and variance). Based on the similarities in the thermal parameter controls (i.e., average flow depth, extent of shading, and similarities in grain sizes), both creeks were expected to be similar at the reach scale.

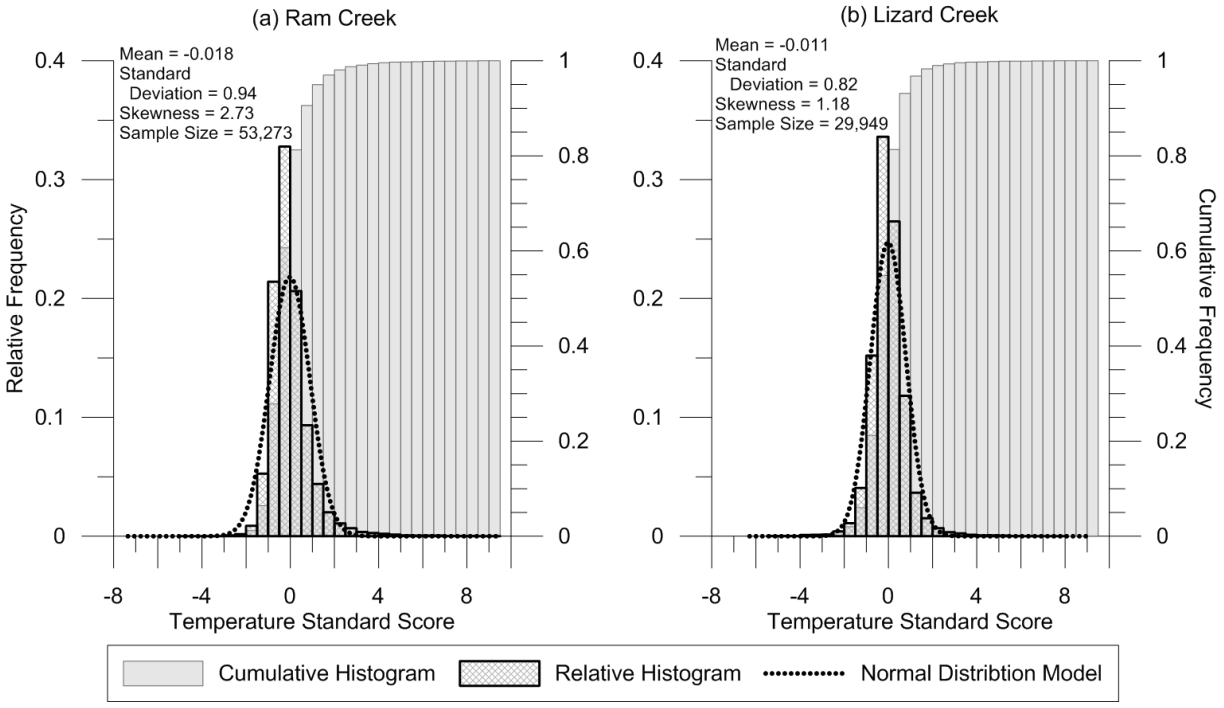

Figure 3-10: Histograms of all the standardized temperature data collected on (a) Ram Creek and (b) Lizard Creek

There is a distinct difference in skewness between the two creeks. Ram Creek has a positive skewness (2.73), indicating that the population is skewed towards the warmer standardized temperatures whereas Lizard Creek has a smaller positive skewness (1.18), representing a more symmetrical distribution as the skewness is closer to zero. Results from parameter cross correlation analysis with depth in Section 3.4.2 indicated that low flow temperatures were warmer at Ram Creek than at Lizard Creek due to warmer atmospheric conditions during the field investigation. Approximately 54% of Ram Creek data was collected at flow depths less than or equal to 0.2 m, indicating that approximately half of the data could have been subject to atmospheric warming. Therefore, the positive skewness of Ram Creek data may be a result of the warm low flow season (July – September) in which data was collected. It was unexpected that Ram Creek would have a warm skewness in temperature distribution as the reach is dominated by bull trout spawning, which has been strongly correlated to cold temperature preferences and therefore, expected to have been a negatively skewed Z_{ijk} distribution (Baxter et al. 2003; Hannah et al. 2004; Warnock et al. 2013).

Cumulative histograms (Figure 3-10) show that, for both study reaches, 90% of standardized temperature data falls between -1.5 and 1.5, and 50% of data falls between -1 and 0.5. Therefore, 50% of the data is within a single standard deviation of the mean temperature, or is between 16% and 69% probability of exceedance of the mean. This confirms the limited variance of the systems that was visually observed within the isotherms in Section 3.4.1. These results provides further support to the necessity of applying statistical analyses of the thermal distributions and equal sampling of both inter- and intra- redd regions, as statistically significant differences could have very similar values, which might be overlooked by a visual analysis.

Z_{ijk} data was spatially binned by morphological feature, which allowed for statistical population comparisons analysis (i.e., t-Test and F-Test) amongst feature classes (pools, riffles and runs) to identify if thermal differences between feature classes were linked to spawning site selection. Means and variances of each feature class are presented in Table 3-3. Results of the population comparison tests and similarities between feature classes are presented in Table 3-4.

Average standardized temperatures of pool and riffles at Ram and Lizard Creek were determined to be significantly different from the other morphological features, and unique within the study reach (i.e., differed from all the data as a whole). For both creeks, normalized temperature averages of pools were warmer than the other features, and averages of riffles were cooler than other features. Redd observations discussed above identified that riffles had limited spawning activity, therefore normalized temperatures within these morphological features were anticipated to be warmer if salmonids were attracted exclusively to colder temperature regions. This observation is also contrary to the fourth-order polynomial

relationships identified in Figures 3-7 and 3-9(a). Here, the current result is in contradiction with the previous results suggest that there are other factors (other than flow depth) that reduce the thermal capacity of the streambed at the riffles. Riffles commonly represent the coarsest fraction of the channel bed material, which would correspond to a lower thermal capacity within the study reach (Barry-Macaulay et al. 2015). Additionally, hyporheic flow emergence has commonly identified within the downstream extents of riffles (Tonina and Buffington 2007). It is possible that groundwater and hyporheic advection energy might be reducing the streambed temperatures within the study reaches, however, groundwater and/or hyporheic exchange was not explicitly quantified during this investigation and therefore cannot be directly linked to the thermal controls.

Table 3-3: Summary of averages and variances of standardized temperature for each feature class

Feature Class	Number of Measurements within Feature Class	Mean Standardized Temperature and Probability of Exceedance	Standardized Temperature Variance
Ram Creek			
All Data	53,273	-0.018 (0.47)	0.89
Pools	17,733	0.043 (0.48)	1.00
Riffles	14,208	-0.076 (0.45)	0.81
Runs	21,332	-0.029 (0.47)	0.85
Within Redds	1,961	-0.171 (0.44)	0.40
Lizard Creek			
All Data	29,949	-0.011 (0.49)	0.67
Pools	9,034	0.027 (0.51)	0.80
Riffles	5,867	-0.063 (0.46)	0.59
Runs	15,066	-0.013 (0.49)	0.64
Within Redds	190	-0.141 (0.46)	0.42

For both study sites, the average and variance of the standardized temperature of the runs were statistically the same as the average of the study reach (Table 3-4). Therefore, average standardized temperature of runs would be an accurate representation of the reach average.

Table 3-4: Summary of statistical analysis completed on standardized temperature populations

Population Comparison	t_{obs}	$t_{\alpha/2,n}$	f_{obs}	$f_{\alpha,dF1,dF2}$
Ram Creek				
POOL vs. All Data	7.05	2.24	1.12	1.02
POOLS vs. RIFFLES	11.14	2.24	1.24	1.03
POOLS vs. RUNS	7.30	2.24	1.17	1.02
POOL vs. REDDS	13.24	2.24	2.48	1.06
RIFFLES vs. All Data	6.79	2.24	1.11	1.02
RIFFLES vs. RUNS	4.76	2.24	1.06	1.03
RIFFLES vs. REDDS	*5.90*	*2.24*	*0.50*	*1.06*
RUNS vs. All Data	***1.51***	***2.24***	***0.96***	***1.02***
RUNS vs. REDDS	9.09	2.24	2.13	1.06
REDDS vs. All Data	10.32	2.24	2.22	1.06
Lizard Creek				
POOL vs. All Data	3.63	2.24	1.16	1.03
POOLS vs. RIFFLES	6.58	2.24	1.28	1.04
POOLS vs. RUNS	3.47	2.24	1.23	1.03
POOL vs. REDDS	3.48	2.26	1.85	1.20
RIFFLES vs. All Data	4.70	2.24	1.10	1.03
RIFFLES vs. RUNS	*4.24*	*2.24*	*1.04*	*1.04*
RIFFLES vs. REDDS	***1.60***	***2.26***	***0.69***	***1.18***
RUNS vs. All Data	***0.17***	***2.24***	***0.94***	***1.02***
RUNS vs. REDDS	2.69	2.26	1.50	1.20
REDDS vs. All Data	2.73	2.26	1.59	1.20
Creek Comparison				
All Data vs. All Data	***1.03***	***2.24***	***0.76***	***1.02***
POOL vs. POOL	***1.31***	***2.24***	***0.78***	***1.03***
RIFFLE vs. RIFFLE	***1.01***	***2.24***	***0.76***	***1.03***
RUN vs. RUN	***1.81***	***2.24***	***0.74***	***1.03***
REDDS vs. REDDS	***0.62***	***2.26***	***1.05***	***1.19***

NOTES:
1. Feature comparison with statistically the same mean are **BOLDED**
2. Feature comparisons with statistically the same variance are in *Italics*

When comparing variance between feature classes, very few similarities were identified; as mentioned above, runs were identified to be statistically the same as the entire dataset, and at Lizard Creek riffles and runs also had statistically the same variance. This suggests that the parameters controlling variability of streambed temperatures are feature class dependent. Flow depth was previously identified as a controlling factor, which is also feature class dependent (i.e., riffles have the lowest flow depths and pools have the deepest flow depth). As suggested above, groundwater and hyporheic flow advection has commonly been linked to morphological features, and may also control the variance of streambed temperature but was not explicitly differentiated in this study.

Relationships between distributions of morphologic feature classes and thermal measurements explicitly within redds were also examined similar to above. Data from Ram Creek indicated that average standardized temperatures of redds were statically colder than all the feature classes and the entire dataset. This further confirms the results observed within the parameter comparison analysis, (i.e., that redds are constructed within in below average temperatures for a given flow depth). It was noted that variance of standardized temperatures of redds was statistically the same as for riffles. As only 4% of all the spawning occurred on riffles, it was unexpected to find statistically significant similarities between the riffles and redds. The variance of the standardized temperatures within the riffles (0.81) is approximately twice as large as the variance of the standardized temperatures within the redds (0.40). Therefore it is likely that this large difference in sample sizes (n = 14,208 and n = 1,961 for the measurements within the riffles and redds respectively) could affect the accuracy of the results. Data from Lizard Creek presented the same results as Ram Creek, with the exception that the redds dataset was determined to have statistically the same average and variance in standardized temperatures as the riffles. No spawning was observed on riffles at Lizard Creek, therefore similarities between riffles and redds was unexpected. Again, it is possible that these results are a product of significantly different sample sizes.

Statistical population comparison of morphological features was also completed between the two study sites (e.g., pools from Ram Creek compared to the pools from Lizard Creek). It was observed that the average and variance of the standardized temperatures of the pools, riffles, runs and redds were statistically the same between both creeks. Therefore, this would suggest that observations made regarding each feature class are not unique to the system, but might be broader and could be potentially applicable to other cobble bed rivers having similar morphology.

Thermal distribution of each morphological feature was compared to the other features within the same class (i.e., Pool 1 compared to Pool 2, etc.). Physical parameters and spawning characteristics (i.e., ρ, ρ_A, and ρ_R) of each feature were compared to determine potential physical thermal controls in attempts to narrow the focus of the preferable thermal spawning regimes on specific features. LSD testing was completed to determine which features had statistically the same average temperatures. Features with statistically the same average as the warmest and coldest features were identified.

At Ram Creek, pools and runs with the hottest normalized temperatures (or with statistically the same average standardized temperature as the hottest pool or run) had the most repeatable and highest density of spawning activities (Table 3-5). It was predicted that colder temperatures would be encountered on features with significant spawning at Ram Creek, based on the previously discussed spawning preferences, therefore these results were unexpected. It is noted that spawning was not exclusive to the warmest features, and spawning with lower ρ, ρ_A, and ρ_R values were observed on several other features,

including the coldest. At Lizard Creek no dominant spawning pattern was found related to any specific feature (Table 3-6). This result can likely be attributable to the small number of redds observed at this site. Spawning dominated on the warmest features contradicts previous results (parameter comparison and feature class comparison) which indicated that spawning occurs within statistically colder sections of the study reach.

Contrary to what was observed in Section 3.4.2, correlations between average flow depth of features and respective temperature is not correlated at Ram Creek based upon LSD testing (Table 3-5) as the warmest and coolest feature have similar flow depths. However, at Lizard Creek, deepest pools and runs are clearly the coldest features (Table 3-6). Again it is possible that other processes contributing to the thermal energy flux of the streambed (such as groundwater emergence or hyporheic exchange) are significantly contributing to thermal energy.

Some pools and runs did not have any spawning during the three years of observations, therefore comparisons between length, slope and area of these specific features and riffles (where spawning essentially did not occur) were assessed. However, no similarities between any of these metrics were identified at either site, largely because riffles were much steeper than any other feature.

Table 3-5: Summary of average thermal measurements, physical characteristics and spawning patterns at Ram Creek, sorted by average Z_{ijk} value. Features statically the same as the coldest feature are highlighted in blue and feature statistically the same as the warmest feature are highlighted in red.

Feature Number		Average Z_{ijk}	Standard Deviation of Z_{ijk}	Physical Characteristics				Spawning Characteristics		
				Average Flow Depth (m)	Length of Feature (m)	Average Slope (%)	Area (m^2)	Average ρ_A	Average ρ	Average ρ_R
Pools	4	-0.20	0.56	0.27	17	0.6%	59	2.5	5.0	1.0
	7	-0.12	0.73	0.28	14	0.6%	50	0.0	0.0	0.0
	6	0.02	0.98	0.16	43	0.2%	185	0.0	0.0	0.0
	3	0.02	1.24	0.29	18	0.2%	121	1.0	2.0	1.0
	5	0.04	1.02	0.27	74	0.3%	582	3.6	4.1	0.3
	2	0.05	1.02	0.19	46	0.4%	455	4.8	5.0	0.0
	1	0.16	0.91	0.26	20	0.2%	194	5.0	10.5	1.0
Riffles	1	-0.18	0.77	0.16	18	2.3%	178	0.0	0.0	0.0
	4	-0.17	0.81	0.20	17	1.7%	262	2.0	3.0	0.8
	2	-0.13	0.55	0.17	18	2.7%	162	0.0	0.0	0.0
	3	-0.09	0.77	0.15	26	2.8%	344	0.0	0.0	0.0
	8	-0.03	0.91	0.21	27	2.0%	202	2.0	2.0	0.0
	7	0.06	0.92	0.15	15	2.5%	60	2.0	2.0	0.0
	6	0.14	1.06	0.20	13	2.5%	89	0.0	0.0	0.0
	5	0.17	0.69	0.16	12	2.3%	118	0.0	0.0	0.0
Runs	5	-0.18	0.86	0.23	11	0.4%	26	0.0	0.0	0.0
	1	-0.09	0.93	0.19	21	1.0%	244	2.7	4.4	1.0
	4	-0.08	0.77	0.22	26	0.8%	185	0.0	0.0	0.0
	3	-0.06	0.91	0.18	32	0.8%	321	3.9	6.9	0.9
	2	-0.01	0.75	0.22	45	0.6%	384	8.0	10.6	0.8
	8	0.01	0.88	0.22	79	0.5%	547	7.2	17.7	1.8
	6	0.02	0.91	0.14	26	0.8%	77	1.0	2.0	1.0
	7	0.03	0.78	0.36	20	0.6%	76	0.0	0.0	0.0

Table 3-6: Summary of average thermal measurements, physical characteristics and spawning patterns at Lizard Creek, sorted by average Z_{ijk} value. Features statically the same as the coldest feature are highlighted in blue and feature statistically the same as the warmest feature are highlighted in red.

	Feature Number	Average Z_{ijk}	Standard Deviation of Z_{ijk}	Physical Characteristics				Spawning Characteristics		
				Average Flow Depth (m)	Length of Feature (m)	Average Slope (%)	Area (m^2)	Average ρ_A	Average ρ	Average ρ_R
Pools	6	-0.09	0.65	0.31	25	0.7%	65	0.0	0.0	0.0
	3	-0.08	0.67	0.31	20	0.6%	59	2.0	2.0	0.0
	4	-0.02	0.92	0.17	34	0.7%	249	2.0	2.0	0.0
	5	0.01	0.67	0.22	32	0.3%	207	1.7	3.0	1.0
	2	0.06	0.74	0.19	42	1.0%	178	0.0	0.0	0.0
	1	0.80	0.26	0.17	22	0.9%	41	0.0	0.0	0.0
Riffles	10	-0.27	0.68	0.12	19	0.7%	96	0.0	0.0	0.0
	9	-0.23	0.17	0.12	9	2.1%	103	0.0	0.0	0.0
	6	-0.15	0.50	0.10	11	1.9%	68	0.0	0.0	0.0
	7	-0.14	0.34	0.14	16	3.0%	125	0.0	0.0	0.0
	1	0.00	0.44	0.16	4	5.7%	52	0.0	0.0	0.0
	3	0.10	0.86	0.19	15	2.5%	83	0.0	0.0	0.0
	4	0.10	0.90	0.15	10	4.2%	70	0.0	0.0	0.0
	2	0.17	0.88	0.08	6	1.8%	41	0.0	0.0	0.0
	8	0.49	1.47	0.17	8	3.7%	37	0.0	0.0	0.0
Runs	5	-0.28	0.59	0.29	12	0.6%	64	0.0	0.0	0.0
	4	-0.14	0.85	0.26	20	0.5%	61	0.0	0.0	0.0
	1	-0.11	0.81	0.24	16	0.9%	86	0.0	0.0	0.0
	3	-0.01	0.60	0.22	27	0.1%	126	0.0	0.0	0.0
	8	-0.01	0.72	0.19	68	0.8%	382	2.3	4.0	1.0
	2	0.01	0.68	0.14	43	0.4%	187	2.3	3.7	1.0
	6	0.07	0.65	0.22	15	0.1%	80	0.0	0.0	0.0
	7	0.08	0.22	0.13	22	0.9%	205	0.0	0.0	0.0

As the results presented in Section 3.4.2 and Table 3-4 contradicted the results in Tables 3-5 and 3-6, further comparisons were necessary to investigate potential correlations previously identified between redds and colder streambed locations (Evans and Petts 1997; Baxter and Hauer 2000; McMahon et al. 2007). Statistical population comparisons (t-Tests and F-Tests) were completed for the features with spawning, to identify differences between standardized temperature distributions of areas selected for spawning versus the entire feature thereby undertaking an inter- and intra-redd comparison (Table 3-7). Locations of all redds, from each year of the surveys were included as they were assumed to represent the desired spawning locations by the animals.

Table 3-7: Comparison of measurements within redds to the entire feature

Population Comparison	**Feature Sample Size**	**Redds[3] Sample Size**	**Feature mean Z_{ijk}**	**Redds[3] Mean Z_{ijk}**	t_{obs}	$t_{\alpha/2,n}$	f_{obs}	$f_{\alpha,dF1,dF2}$
Ram Creek								
POOL-1	**1862**	**284**	**0.16**	**0.23**	**1.93**	**2.25**	**3.14**	**1.17**
POOL-2	5026	97	0.05	-0.10	3.42	2.27	5.57	1.29
POOL-3	1039	19	0.02	-0.35	6.04	2.33	24.90	1.92
POOL-4	541	96	-0.20	-0.54	7.03	2.25	4.81	1.31
POOL-5	6822	142	0.04	-0.13	3.79	2.26	3.52	1.23
RIFFLE-4	**2768**	**78**	**-0.17**	**-0.27**	**1.33**	**2.28**	**2.16**	**1.34**
RIFFLE-7	**537**	**11**	**0.06**	**0.02**	**0.27**	**2.59**	**3.20**	**2.55**
RIFFLE-8	2324	17	-0.03	0.31	3.02	2.46	4.31	2.01
RUN-1	**2923**	**77**	**-0.09**	**-0.18**	**1.22**	**2.28**	**2.18**	**1.34**
RUN-2	4528	195	-0.01	-0.20	5.14	2.26	3.07	1.20
RUN-3	**3362**	**113**	**-0.06**	**-0.10**	**0.44**	**2.27**	**1.40**	**1.27**
RUN-6	675	25	0.02	-0.84	17.80	2.27	37.32	1.74
RUN-8	6926	801	0.01	-0.26	10.26	2.24	1.95	1.09
Lizard Creek								
POOL-3	460	27	-0.08	-0.54	4.03	2.35	2.07	1.71
POOL-4	**3088**	**15**	**-0.02**	**0.01**	**0.24**	**2.49**	**4.01**	**2.13**
POOL-5	2294	78	0.01	-0.22	3.70	2.28	2.51	1.34
RUN-2	***2361***	***14***	***0.01***	***0.37***	***2.43***	***2.53***	***2.21***	***2.21***
RUN-8	***5388***	***51***	***-0.01***	***0.03***	***0.37***	***2.31***	***1.09***	***1.44***

NOTES:
1. Feature comparison with statistically the same mean are **BOLDED**
2. Feature comparisons with statistically the same variance are in *Italics*
3. "Redds" refers to the measurements taken within the limits of the previously surveyed redds

Of the 13 morphologic features on Ram Creek that experienced spawning, five features with redds were determined to have statistically the same average standardized temperature as the entire feature in which redds were observed. None of the features with redds have the same variance as the feature in which they

were observed within. It is noted that there is a large difference in the sample sizes of the features and the redd datasets, which could affect the accuracy of t-Tests and F-Tests. With the exception of Pool-1 and Riffle-8, average standard temperature of the measurements within redds was lower than the average of the feature in which redds were observed.

Of the five spawning features on Lizard Creek, three of the features with spawning had statistically the same mean, and of these, two had statically the same variance as the entire feature. It was noted that average redd temperatures were colder than the average feature temperature, for those features determined to be statistically different. Conversely, redds on the three remaining features demonstrated slightly warmer average temperatures (although considered statistically the same) than the features in which redds were observed. Again, it is noted that there are large differences in sample sizes which could affect the accuracy of the tests.

The series of statistical population comparisons provided strong evidence that redds at Ram Creek were dominantly constructed within the coldest sections of features with the warmest average streambed temperature. However, this analysis may be prone to some errors as there is a large difference between the sample sizes of the data collected within a redd and within a feature, which is a result of the large difference in size between the two areas. To determine if redds are spatially correlated to the coldest locations a SAC analysis was completed to provide a quantitative representation of the spatial relationship.

3.4.4 SAC Analysis with Proximal Redd Spatial Correlations

The G_i^* SAC analysis resulted in a series of identified hot and cold spots along both study reaches (Table 3-8). At Ram Creek, 9 redds (9% of all redds observed) were within the limits (super-positioned) of the hot spots, and 27 redds (26%) were within the limits of cold spots. At Lizard Creek, 6 redds (40% of all redds observed) were within the limits of the hot spots, and 3 redds (20%) were within the limits of cold spots. There were, however no correlations between ρ_A, ρ, and ρ_R values of redds associated with significant spots, as the full range of all three metrics were observed for redds within the significant areas.

Table 3-8: Summary of significant spot characteristics from both Ram and Lizard Creek

Study Area	Characteristic	Hot	Cold
Ram Creek	Number of spots (% of total)	93 (44%)	119 (56%)
	Average area (m^2)	4.63	4.23
	Average standardized temperature	1.17	-0.86
	Number of redds within spot	9 (9%)	27 (26%)
	Number of redds with significant R_i	2 (2%)	16 (16%)
Lizard Creek	Number of spots	60 (51%)	57 (49%)
	Average area (m^2)	4.09	4.21
	Average standardized temperature	0.85	-0.83
	Number of redds within spot	6 (40%)	3 (20%)
	Number of redds with significant R_i	2 (13%)	3 (20%)

The redd proximity metric (R_i) was calculated to determine correlations between significant spots and redds; R_i evaluates the significance of all the cold and hot spots near or encompassing the redds in question and is summarized in Table 3-8. R_i analysis identified half as many redds as significantly correlated to cold spot, relative to the number of redds within significant spots. At Ram Creek, only 18 of the 103 individual spawning locations were determined to be correlated to significant spot, and only 16 were correlated to cold spots. This suggests that the majority of redds (84%) are not correlated to cold spots. At Lizard Creek 80% of redds were not correlated to cold spots.

When redds at Ram Creek were stratified by ρ, ρ_A, and ρ_R, results showed that redds with significant R_i were located in areas with the highest ρ, ρ_A, and ρ_R values within the entire study area. Of the 16 redds correlated to cold spots, 11 (69%) occurred where $\rho_A \geq 8$ and 13 (81%) where $\rho \geq 10$. Furthermore, all redds have a minimum ρ_R of 1, indicating that the area was used for spawning two years out of the three analyzed. Therefore, R_i analysis at Ram Creek, indicate that redds found in the proximity to cold spots,

are redds within the most desirable spawning areas. Figure 3-11 shows the distributions of the annual and cumulative densities of redds with significant R_i, redd located within cold spots, and all other redds.

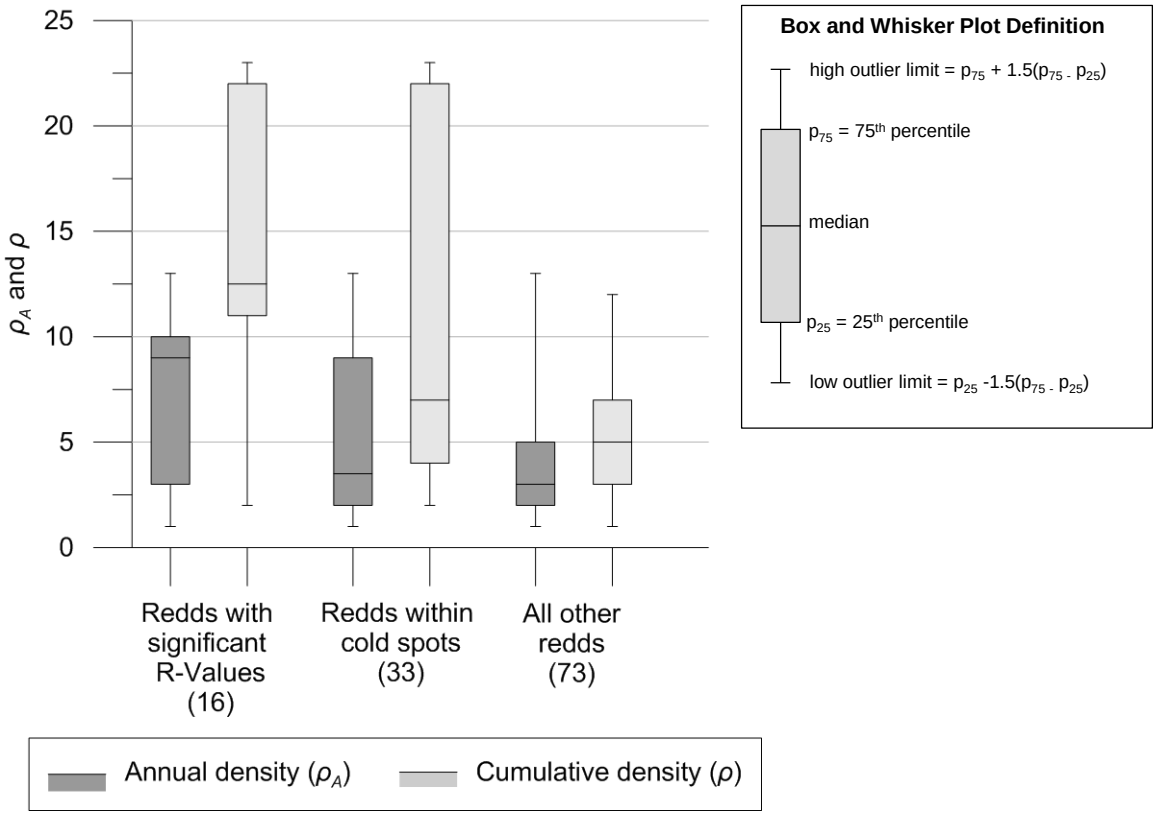

Figure 3-11: Comparison of the redd annual density and ρ identifying the type of correlation to cold spots at Ram Creek.

Redds with significant R_i have higher p_{75}, p_{50} (median), and p_{25} ρ_A values than redds found within cold spots, or over all other redds observed (Figure 3-11). Redds with significant R_i also have the highest median ρ. As previously observed in the G_i* analysis, redds superimposed within the cold spots have a large range in ρ and redds with significant R_i have higher median and p_{25} values. Furthermore, the median and p_{75} values of ρ for redds within cold spots are larger than the corresponding values found for the whole dataset. These results add further evidence that redds within close proximity of the most significant cold spots represent the densest and most frequented spawning areas within the study reach.

Median values and overall data range of ρ_A within cold spots is approximately equal to all the other redds although p_{75} is larger for the former. Therefore the redds superimposed within the cold areas did not represent the most significant spawning areas (with the highest ρ_A, ρ and ρ_R). The results of the SAC analysis compliment the results found with the statistical population analysis that the redds are correlated to the colder areas within the study reach.

3.5 Discussion

Groundwater and hyporheic flow emergence may be a dominant process affecting the locations of isolated cold spots, however, this was not explicitly quantified during the current investigation. For both study reaches, normalized average streambed temperatures of riffles were determined to be statistically cooler than other features. Based on the relationship established within the parameter cross correlation, warmer temperatures would be expected to occur on the feature with the lowest flow depths (i.e., riffles and runs). Therefore, as this was not observed with the riffle, it is expected that there are other factors reducing the thermal capacity of the streambed at the riffles. Groundwater or hyporheic flow emergence has commonly identified within the downstream extents of riffles (Tonina and Buffington 2007; Tonina and Buffington 2009) and it is possible that groundwater and hyporheic advection energy might be reducing the streambed temperatures within the study reaches. Furthermore, streambed temperature variance was determined to be statistically different between most feature classes. This suggests that the parameters controlling variability of streambed temperatures are feature classes dependent. As the groundwater and hyporheic flow have a reduced range in temperature fluctuations (relative to the surface water temperature) it is plausible that the areas with the least variance (i.e., the riffles) have significant groundwater or hyporheic flow contributions to the streambed.

It is possible that several of the cold spots identified with the SAC analysis could be the result of groundwater or hyporheic flow emergence. Approximately 100 significant cold spots were identified on each study reach using the SAC analysis. Unfortunately, traditional methods of quantifying groundwater emergence, such as piezometers (Conant 2001), seepage meters (Rosenberry 2008) or streambed thermal profiling (Stonestrom and Constantz 2003; Kim et al. 2014), required resources beyond the limits and of the current study. If the HI-RES TMD were modified to incorporate a secondary measurement to confirm the presence of groundwater or hyporheic flow emergence then secondary investigations would not be necessary.

Several water quality parameters differ between groundwater and surface water (e.g., conductivity, dissolved oxygen, pH) and have been used as natural tracers to study submerged flow for several decades (Anderson 2005; Kalbus et al. 2006; Cardenas 2015). By incorporating one of these measurements into the HI-RES TMD, groundwater and hyporheic flow emergence could be identified by cross correlation of spatial variability of streambed temperatures and chemistry. As bull trout spawning site selection has been frequently linked to groundwater emergence, employing additional measurement techniques to differentiate surface waters from groundwater relative to the local geochemical conditions may add considerable insight into the spatial analysis observations as a future tool.

3.6 Conclusions and Recommendations

A series of temperature measurements (n > 80,000) were collected using a recently developed high-resolution thermal array (HI-RES TMD) in two cobble bed rivers of southeastern BC. Spawning surveys were completed with the assistance of experienced fisheries biologist during the falls of 2012, 2013, and 2014 and springs of 2013 and 2014 to identify bull trout and cutthroat trout redds. Isotherm maps were created for both study sites to visually analyze the streambed temperature distributions at each site. The isotherms did not visually show any positive or negative correlation between the clustering of the streambed temperatures and the redd locations. As the dataset presented here provides unprecedented resolution and extent of cover of streambed thermal measurements, it is unlikely, based upon the current study, that significant spatial correlations between streambed thermal distribution and redds can be reliably identified solely with visual analysis. This analysis was also used to determine suitable methods of analysis based on the clustering and variance of the data.

Parameter cross correlation and analysis of the skewness of the temperature distributions showed that areas with flow depth less than 0.2 m where affected by atmospheric warming, and streambed temperatures at these locations were dominantly controlled by sensible and latent thermal energy flux. A series of statistical population comparisons provided strong evidence that redds at Ram Creek were dominantly constructed within the coldest sections of the features with the warmest average streambed temperature. As much of the study area was determined to have limited localized temperature variance, the warmest average features would have the largest thermal contrasts, which would make colder locations easier to identify. Therefore, it is possible that spawning sites are not correlated to the warmer features, just features where colder areas are more readily experienced by the animals. This correlation between colder temperatures and redds was not as evident within the Lizard Creek data, however, this may be a product of the smaller number of redds observed and a different species in fish (cutthroat trout) which may be seeking out different streambed conditions.

Morphological binning identified similarities between study sites. Thermal morphological observations included:

1. Pools having slightly warmer average standardized streambed temperature than riffles,
2. Runs representative of the average reach standardized streambed temperature,

Similarities within the redd locations and the features were also observed:

3. Bull trout and cutthroat trout seek the similar average standardized streambed temperatures,

It is possible that these trends are applicable to other plane-bed, cobble/gravel systems, however, further monitoring of more sites would be necessary to confirm the patterns.

It was unexpected that riffles would have the coldest average temperatures amongst the features as parameter cross correlation indicated that shallower flows have warmer temperatures, and riffles are characteristic of having low flow. Therefore, this would indicate that there are other factors (besides flow depth), that reduce thermal capacity of the streambed at the riffles. Riffles commonly represent the coarsest fraction of the channel bed material, which would represent lower thermal capacity within the study reach. Additionally, hyporheic flow emergence has commonly identified within the downstream extents of riffles, therefore, it is plausible that groundwater and hyporheic advection energy might be reducing the streambed temperatures within the study reaches. Groundwater or hyporheic exchange was not quantified during this investigation and therefore cannot be explicitly linked to the thermal controls.

SAC analysis coupled with the redd proximity metric determined that redds with the highest ρ_A, ρ or ρ_R were correlated to cold spots within Ram Creek study area. However, redds with significant correlation to cold spots represent only 16% of redds observed within the study reach, indicating that most redds were not correlated to cold spots. It is not possible to know whether site selection preference identified here is directly related to cold spots or to other parameters causing their occurrence (e.g., groundwater emergence). However, it is not expected that the remaining redds are randomly located within the channel, and secondary or tertiary spawning site selection characteristics might be correlated to a larger percentage of the surveyed redds. Correlations to other information collected during field investigations (e.g., grain size distributions, woody debris, and vegetation within the channel) might provide insight to secondary spawning site selection preferences. Further SAC analysis of this dataset might provide further insight into spawning habitat selection.

The spatial analysis conducted to correlate cold spots and redds was only possible because of the extent and resolution of the field measured data. The sub-meter resolution of the data, covering several sequential morphological features, was able to convey the variance of streambed temperatures, define morphological thermal trends and isolate areas of significantly different temperatures. The HI-RES TMD system employed here was able to overcome the constraints of previously used streambed temperature measurement methods, and with the accompaniment of temperature normalization, provided an unprecedented dataset resolution. Implementation of the system on additional spawning rivers will provide a stronger foundation for comparison of thermal streambed patterns, which might add insight to the effects of morphology on the controls of thermal distribution of the streambed.

Conclusions

A series of temperature measurements (n > 80,000) were collected using a recently developed high-resolution thermal array (HI-RES TMD) in two cobble bed rivers of southeastern BC. Spawning surveys were completed with the assistance of experienced fisheries biologist during the falls of 2012, 2013, and 2014 and springs of 2013 and 2014 to identify bull trout and cutthroat trout redds. The HI-RES TMD system was developed to sample streambed interface temperatures at high resolution. The equipment was employed during low flow conditions to sample multiple morphologic units at unprecedented resolution. Being that the equipment deployment non-invasive, no negative impacts to aquatic habitat occurred as a result of the sampling method.

Isotherm maps were created for both study sites to visually analyze the streambed temperature distributions at each site. A visual analysis of the isotherms did not show any positive or negative correlation between the clustering of the streambed temperatures and the redd locations. However, this may be due to the unprecedented resolution and extent of cover of streambed thermal measurements.

Most of the redds at Ram Creek were constructed within the coldest spots of features characterized by the warmest average streambed temperature. As much of the study area was determined to have limited localized temperature variance, the warmest average features would have the largest thermal contrasts, which would make colder spots located within them easier to identify by salmonids. This was not as evident with the Lizard Creek data, although this may be caused by the smaller number of redds observed (15 verses 103) or by the different species of fish encountered there (cutthroat trout vs bull trout). Furthermore bull trout and cutthroat trout seek similar average standardized streambed temperatures and seek spawning areas with temperature distributions. Nevertheless, they avoid spawning on riffles.

SAC and redd proximity metric analysis determined that redds with the highest density, (annual and cumulative) and repeatability were correlated to cold spots within Ram Creek study area. Redds with significant correlation to cold spots represent only 16% of redds observed within the study reach. Thus, a larger percentage of the surveyed redds might be correlated to secondary or tertiary spawning site selection characteristics. Correlations to other information collected during field investigations (e.g., grain size distributions, woody debris, and vegetation within the channel) might provide insight to secondary spawning site selection preferences.

Data collected by HI-RES TMD was also analyzed through morphological binning. It was found that pools are slightly warmer than riffles and that runs have similar streambed temperature than the average

of the whole reach. Shallow areas (less than 0.2 m depth) were found to be affected by atmospheric warming through a parameter cross correlation and analysis of the skewness of the temperature distributions. Therefore, as riffles have shallow depths, especially at low flow, it was unexpected that they would have the coldest average temperatures amongst the features. This would indicate that there are other factors, affecting streambed temperatures on riffles. Coarse material, found on riffles and not in pools has lower thermal capacity. Furthermore, it is possible that hyporheic flow emergence, commonly identified within the downstream extents of riffles, was occurring. Unfortunately, groundwater or hyporheic exchange was not quantified during this investigation and therefore cannot be explicitly linked to the thermal controls. It is possible that these trends are applicable to other plane-bed, cobble/gravel systems; however, further monitoring of more sites would be necessary to confirm the patterns.

On a final note, all the spatial analyses and temperature mapping presented in this document were only possible because of the extent and resolution of the field measured data. The HI-RES TMD system was designed to overcome the constraints of previously used streambed temperature measurement methods. The sub-meter resolution of the data and the post-processing techniques adopted were able to portray the variance of streambed temperatures, define morphological thermal trends and isolate areas of significantly different temperatures. Implementation of the HI-RES TMD on other watercourses will provide a stronger foundation for comparison of thermal streambed patterns, based on morphological features, grain size distribution, flow depth or other factors.

References

Albert DP, Gesler WM, Levergood B. 2000. Spatial analysis, GIS and remote sensing: applications in the health sciences. Ann Arbor: Sleeping Bear Press.

Anderson MP. 2005. Heat as a ground water tracer. Groundwater. 43:951–68.

Annable WK. 1996. Morphologic relationships of rural watercourses in southern Ontario and selected field methods in fluvial geomorphology. Waterloo, ON: Ontario Ministry of Natural Resources.

Barry-Macaulay D, Bouazza A, Wang B, Singh RM. 2015. Evaluation of soil thermal conductivity models. Canadian Geotechnical Journal. 52:1–9.

Baxter C, Hauer FR, Woessner WW. 2003. Measuring groundwater stream water exchange: new techniques for installing minipiezometers and estimating hydraulic conductivity. Transactions of the American Fisheries Society. 132:493–502.

Baxter C, Hauer FR. 2000. Geomorphology, hyporheic exchange, and selection of spawning habitat by bull trout (Salvelinus confluentus). Canadian Journal of Fisheries and Aquatic Sciences. 57:1470–1481.

Baxter JS, McPhail JD. 1997. Diel microhabitat preferences of juvenile bull trout in an artificial stream channel. North American Journal of Fisheries Management. 17:975–980.

Bencala K. 2000. Hyporheic zone hydrological processes. Hydrological Processes. 14:2797–2798.

Beschta RL. 1997. Riparian shade and stream temperature: an alternative perspective. Rangelands. 19:25–28.

Bickel TO, Closs GP. 2008. Impact of Didymosphenia geminata on hyporheic conditions in trout redds: reason for concern? Marine and Freshwater Research 59:1028–1033.

Brown L, Hannah D. 2008. Spatial heterogeneity of water temperature across an alpine river basin. Hydrological Processes. 22:954–967.

Bunn SE, Davies PM, Mosisch TD. 1999. Ecosystem measures of river health and their response to riparian and catchment degradation. Freshwater Biology. 41:333–345.

Burkholder B, Grant G, Haggerty R, Khangaonkar T, Wampler P. 2008. Influence of hyporheic flow and geomorphology on temperature of a large, gravel-bed river, Clackamas River, Oregon, USA. Hydrological Processes. 22:941–953.

Burner CJ. 1951. Characteristics of spawning nests of Columbian River salmon. Fishery Bulletin of the Fish and Wildlife Service. 52:97–110.

Buss S, Cai Z, Cardenas B, Fleckenstein J, Hannah D. 2009. The hyporheic handbook: a handbook on the groundwater-surfacewater interface and hyporheic zone for environmental managers.

Caissie D. 2006. The thermal regime of rivers: a review. Freshwater Biology. 51:1389–1406.

Cardenas BM. 2015. Hyporheic zone hydrologic science: A historical account of its emergence and a prospectus. Water Resources Research. 51:3601–3616.

Carrivick J, Brown L, Hannah D, Turner A. 2012. Numerical modelling of spatio-temporal thermal heterogeneity in a complex river system. Journal of Hydrology. 414-415:491–502.

Chanson H. 2004. Environmental Hydraulics of Open Channel Flows. Burlington, MA: Elsevier Butterworth-Heinemann.

Collier M. 2008. Demonstration of fiber optic distributed temperature sensing to differentiate cold water refuge between ground water inflows and hyporheic exchange. Corvallis, Oregon: Oregon State University.

Conant B. 2001. A PCE plume discharging to a river: Investigations of flux, geochemistry, and biodegradation in the streambed. Waterloo, ON: University of Waterloo, Department of Earth Science.

Conant B. 2004. Deliniation and quantifying ground water discharge zones using streambed temperatures. Groundwater. 42:243–257.

Constantz J. 1998. Interaction between stream temperature, streamflow, and groundwater exchanges in alpine streams. Water Resources Research. 34:1609–1615.

Côté J, Konrad JM. 2005. Thermal conductivity of base-course materials. Canadian Geotechnical Journal. 42:61–78.

Dale RK, Miller DC. 2007. Spatial and temporal patterns of salinity and temperature at an intertidal groundwater seep. Estuarine, Coastal and Shelf Science. 72:283-298

Duarte T, Hemond HF, Frankel D. 2006. Assessment of submarine groundwater discharge by handheld aerial infrared imagery: Case study of Kaloko fishpond and bay, Hawai'i. 4:227–236.

Eckmann M. 2014. Bioenergetic evaluation of diel vertical migration by bull trout . Corvallis, Oregon: Oregon State University.

Edinger JE, Duttweiler DW, Geyer JC. 1968. The response of water temperatures to meteorological conditions. Water Resources Research. 4:1137–1143.

ESRI (2011) ArcGIS Desktop. Release 10. Redlands, CA: Environmental Systems Research Institute.

Evans EC, Petts GE. (1997) Hyporheic temperature patterns within riffles, Hydrological Sciences Journal, 42:2, 199-213

Feio MJ, Alves T, Boavida M, Medeiros A. 2010. Functional indicators of stream health: a river basin approach. Freshwater Biology. 55:1050–1065.

Fraley J, Shepard B. 1989. Life history, ecology and population status of migratory bull trout (Salvelinus confluentus) in the Flathead Lake and River system.

Geist DR, Dauble DD. 1998. Redd site selection and spawning habitat use by fall chinook salmon: the importance of geomorphic features in large rivers. Environmental Management. 22:655–669.

Geist DR. 2000. Hyporheic discharge of river water into fall chinook salmon (Oncorhynchus tshawytscha) spawning areas in the Hanford Reach, Columbia River. Canadian Journal of Fisheries and Aquatic Sciences. 57:1647–1656.

Getis A, Ord JK. 2010. The analysis of spatial association by use of distance statistics. Perspectives on Spatial Data Analysis.127–145.

Golden N, Morrison L, Gibson PJ, Potito AP. 2015. Spatial patterns of metal contamination and magnetic susceptibility of soils at an urban bonfire site. Applied Geochemistry. 52:86–96.

Haining R. 2003. Spatial statistics and the analysis of health data. In: Vol. 6. Taylor & Francis.

Hale JG, Hilden DA. 1969. Spawning and Some Aspects of Early Life History of Brook Trout, Salvelinus fontinalis (Mitchill), in the Laboratory. 98:473–477.

Hannah D, Malcolm I, Soulsby C, Youngson A. 2004. Heat exchanges and temperatures within a salmon spawning stream in the Cairngorms, Scotland: seasonal and sub-seasonal dynamics. River Research and Applications. 20:635–652.

Hannah D, Webb B, Nobilis F. 2008. River and stream temperature: dynamics, processes, models and implications. Hydrological Processes. 22:899–901.

Hanrahan TP. 2007. Bedform morphology of salmon spawning areas in a large gravel-bed river. Geomorphology. 86:529–536.

Hansen EA. 1975. Some effects of groundwater on brown trout redds. Transactions of the American Fisheries Society 104:100–110.

Hendricks SP, White DS. 1988. Hummocking by lotic chara: observations on alterations of hyporheic temperature patterns. 31:13–22.

Hipel KW, McLeod AI. 1994. Time Series Modelling of Water Resources and Environmental Systems. Amsterdam, Netherlands: Elsevier.

Imhol JG, Fitzgibbon J, Annable WK. 1996. A hierarchical evaluation system for characterizing watershed ecosystems for fish habitat. Canadian Journal of Fisheries and Aquatic Sciences. 53:312–326.

Johnson FA. 1971. Stream temperatures in an apline area. Journal of Hydrology. 14:322-336.

Johnson S. 2004. Factors influencing stream temperatures in small streams: substrate effects and a shading experiment. Canadian Journal of Fisheries and Aquatic Sciences. 61:913–923.

Jonsson, B, Jonsson, N. 2011. Ecology of Atlantic salmon and brown trout habitat as a template for life histories. In Fish & Fisheries Series. Vol. 33. Springer.

Kalbus E, Reinstorf F, Schirmer M. 2006. Measuring methods for groundwater surface water interactions: a review. Hydrology and Earth System Sciences. 10:873–887.

Kim H, Lee K-K, Lee J-Y. 2014. Numerical verification of hyporheic zone depth estimation using streambed temperature. Journal of Hydrology. 511:861–869.

Kitano S, Maekawa K, Nakano S, Fausch K. 1994. Spawning behavior of bull trout in the upper Flathead drainage, Montana, with special reference to hybridization with brook trout. Transactions of the American Fisheries Society. 123:988–992.

Knapp RA, Preisler HK. 1999. Is it possible to predict habitat use by spawning salmonids? A test using California golden trout (Oncorhynchus mykiss aguabonita). Canadian Journal of Fisheries and Aquatic Sciences. 56:1576–1584.

Kondolf GM, Wolman MG. 1993. The sizes of salmonid spawning gravels. Water Resources Research. 29:2275-2285

Käser DH, Binley A, Heathwaite AL. 2013. On the importance of considering channel microforms in groundwater models of hyporheic exchange. River Research and Applications. 29:528–535.

Lee J, Wong D. 2001. Statistical analysis with ArcView GIS. Wiley.

Leopold LB, Wolman GM, Miller JP. 2012. Fluvial processes in geomorphology. Courier Dover Publications, Mineola.

Levec F, Skinner A. 2004. Manual of instructions bathymetric surveys. Ministry of Natural Resources.

Lisle T. 1987. Using "residual depths" to monitor pool depths independently of discharge. U.S. Department of Agriculture.

Lisle TE, Lewis J. 1992. Effects of sediment transport on survival of salmonid embryos in a natural stream: a simulation approach. Canadian Journal of Fisheries and Aquatic Sciences. 49:2337–2344.

Loheide SP, Gorelick SM. 2006. Quantifying stream-aquifer interactions through the analysis of remotely sensed thermographic profiles and in situ temperature histories. Environmental Science & Technology. 40:3336–3341.

Lounder V. 2011. Temporal and spatial hydrodynamic variability in a gravel-bed river: measurement, characterisation, and significance for spawning salmonids. Waterloo: University of Waterloo.

Malcolm, Soulsby, Youngson, Petry. 2003. Heterogeneity in ground water–surface water interactions in the hyporheic zone of a salmonid spawning stream. Hydrological Processes. 17:601–617.

Marchildon, Annable, Imhof, Power. 2011. A high-resolution hydrodynamic investigation of brown trout (Salmo trutta) and rainbow trout (Oncorhynchus mykiss) redds. River Research and Applications. 27:345–359.

Marchildon MA, Annable WK, Power M, Imhof JG. 2012. A hydrodynamic investigation of brown trout (Salmo trutta) and rainbow trout (Oncorhynchus mykiss) redd selection at the riffle scale. River Research and Applications. 28:659–673.

Marchildon MA. 2009. A high-resolution hydrodynamic investigation of brown trout (salmo trutta) and rainbow trout (salmo gairdneri) redds. Waterloo: University of Waterloo.

McMahon TE, Zale AV, Barrows FT. 2007. Temperature and competition between bull trout and brook trout: a test of the elevation refuge hypothesis. Transactions of the American Fisheries Society. 136:1313–1326.

Meyer JL. 1997. Stream health: incorporating the human dimension to advance stream ecology. Journal of the North American Benthological Society. 16:439–447.

Mohamad IB, Usman D. 2013. Standardization and its effects on k-means clustering algorithm. Research Journal of Applied Sciences, Engineering and Technology. 6:3299–3303.

Montgomery D, Buffington J. 1997. Channel-reach morphology in mountain drainage basins. Geological Society of America Bulletin. 109:596–611.

Moore RD, Nelitz M, Parkinson E. 2013. Empirical modelling of maximum weekly average stream temperature in British Columbia, Canada, to support assessment of fish habitat suitability. Canadian Water Resources Journal. 38:1–13.

Moore RD. 2006. Stream Temperature Patterns in British Columbia, Canada, Based on Routine Spot Measurements. 31:41–56.

Muhlfeld CC. 2002. Spawning characteristics of redband trout in a headwater stream in Montana. North American Journal of Fisheries Management.

Mull KE, Wilzbach MA. 2007. Selection of spawning sites by coho salmon in a northern California stream. North American Journal of Fisheries Management. 27:1343–1354.

Ochsner TE, Horton R, Ren T. 2001. A new perspective on soil thermal properties. Soil Science Society of America Journal. 65:1641–1647.

Preud'Homme EB, Stefan HG. 1992. Errors related to random stream temperature data collection in upper Mississippi River watershed. Journal of the American Water Resources Association. 28:1077-1082.

Rieman B, McIntyre JD. 1993. Demographic and habitat requirements for conservation of bull trout. Ogden, UT: United States Department of Agriculture, Forest Service, Intermountain Research Station.

Rieman BE, McIntyre JD. 1996. Spatial and temporal variability in bull trout redd counts. North American Journal of Fisheries Management. 16:132–141.

Ringler NH, Hall JD. 1975. Effects of logging on water temperature, and dissolved oxygen in spawning beds. Transactions of the American Fisheries Society. 104:111–121.

Rosenberry D. 2008. A seepage meter designed for use in flowing water. Journal of Hydrology. 359:118–130.

Rosgen DL. A classification of natural rivers. Catena. 22:169-199

Sabatino DR, Praisner TJ, Smith CR. 2000. A high-accuracy calibration technique for thermochromic liquid crystal temperature measurements. Experiments in Fluids. 28:495–505.

Schmidt C, Bayer-Raich M, Schirmer M. 2006. Characterization of spatial heterogeneity of groundwater-stream water interactions using multiple depth streambed temperature measurements at the reach scale. Hydrology Earth Systems Science. 10:849–859.

Selker JS, Thévenaz L, Huwald H, Mallet A, Luxemburg W, van de Giesen N, Stejskal M, Zeman J, Westhoff M, Parlange MB. 2006. Distributed fiber optic temperature sensing for hydrologic systems. Water Resources Research. 42:1–8.

Stallman R.W. 1965. Steady one-dimensional fluid flow in a semi-infinite porous medium with sinusoidal surface temperature. Journal of Geophysical Research. 70:2821–2827.

Stamp J, Hamilton A, Craddock M, Parker L, Roy A, Isaak D, Holden Z, Bierwagan B. 2013. Best practices for continuous monitoring of temperature and flow in wadeable streams. Washington, DC: United States Environmental Protection Agency, National Center for Environmental Assessment.

Steinhart JS, Hart SR. 1968. Calibration curves for thermistors. Deep Sea Research and Oceanographic Abstracts. 15:497–503.

Stisen S, Sandholt I, Nørgaard A, Fensholt R. 2007. Estimation of diurnal air temperature using MSG SEVIRI data in West Africa. Remote Sensing of Environment. 110:262–274.

Stonestrom DA, Constantz J. 2003. Heat as a tool for studying the movement of ground water near streams. Reston, Virgina: USGS.

Stubbington R, Wood PJ, Boulton AJ. 2009. Low flow controls on benthic and hyporheic macroinvertebrate assemblages during supra-seasonal drought. Hydrological Processes. 23:2252–2263.

Tonina D, Buffington JM. 2007. Hyporheic exchange in gravel bed rivers with pool riffle morphology: Laboratory experiments and three dimensional modeling. Water Resources Research. 43.

Tonina D, Buffington JM. 2009. Hyporheic exchange in mountain rivers I: mechanics and environmental effects. Geography Compass. 3:1063–1086.

de la Torre A, Iglesias I, Carballo M, Ramírez P. 2012. An approach for mapping the vulnerability of European Union soils to antibiotic contamination. Science of the Total Environment. 414:672–679.

Trauth N, Schmidt C, Vieweg M, Oswald SE, Fleckenstein JH. 2015. Hydraulic controls of in stream gravel bar hyporheic exchange and reactions. Water Resources Research. 51:2243–2263.

Trimble Navigation Limited . 2013. Trimble S6 Total Station Data Sheet.

Usowicz B, Lipiec J, Ferrero A. 2006. Prediction of soil thermal conductivity based on penetration resistance and water content or air-filled porosity. International Journal of Heat and Mass Transfer. 49:5010–5017.

Vaux WG. 1967. Intragravel flow and interchange of water in streambed. Fishery Bulletin. 66:479–489.

Vogt T, Schneider P, Hahn-Woernle L, Cirpka O. 2010. Estimation of seepage rates in a losing stream by means of fiber-optic high-resolution vertical temperature profiling. Journal of Hydrology. 380:154–164.

Walpole RE, Myers RH, Myers SL, Ye K. 1993. Probability and statistics for engineers and scientists. 8th. Prentice Hall, Englewood Cliffs, New Jersey.

Wang ZY, Lee J, Melching CS. 2014. River dynamics and integrated river management. Beijing: Springer.

Warnock WG, Rasmussen JB, Magnan P. 2013. Abiotic and biotic factors associated with brook trout invasiveness into bull trout streams of the Canadian Rockies. Canadian Journal of Fisheries and Aquatic Sciences. 70:905–914.

Webb BW, Zhang Y. 1997. Spatial and seasonal variability in the components of the river heat budget. Hydrological Processes. 11:79–101.

White DS, Elzinga CH, Hendricks SP. 1987. Temperature patterns within the hyporheic zone of a northern Michigan River. Journal of the North American Benthological Society. 6:85–91.

White HC. 1930. Some observations of the eastern brook trout of PEI. Transactions of the American Fisheries Society. 60:101–108.

Witzel LD, Maccrimmon HR. 1983. Redd-site selection by brook trout and brown trout in southwestern Ontario streams. Transactions of the American Fisheries Society. 112:760–771.

Wójcik R, Buishand TA. 2003. Simulation of 6-hourly rainfall and temperature by two resampling schemes. Journal of Hydrology. 273:69–80.

Yilmaz A, Shafique K, Shah M. 2003. Target tracking in airborne forward looking infrared imagery. Image and Vision Computing. 21:623–635.

Zakšek K, Oštir K. 2012. Downscaling land surface temperature for urban heat island diurnal cycle analysis. Remote Sensing of Environment. 117:114-124

Zimmer MA, Power LK. 2006. Brown trout spawning habitat selection preferences and redd characteristics in the Credit River, Ontario. Journal of Fish Biology. 68:1333–1346.

Appendices

Appendix A: Temperature Probe Calibration and Validation Curves

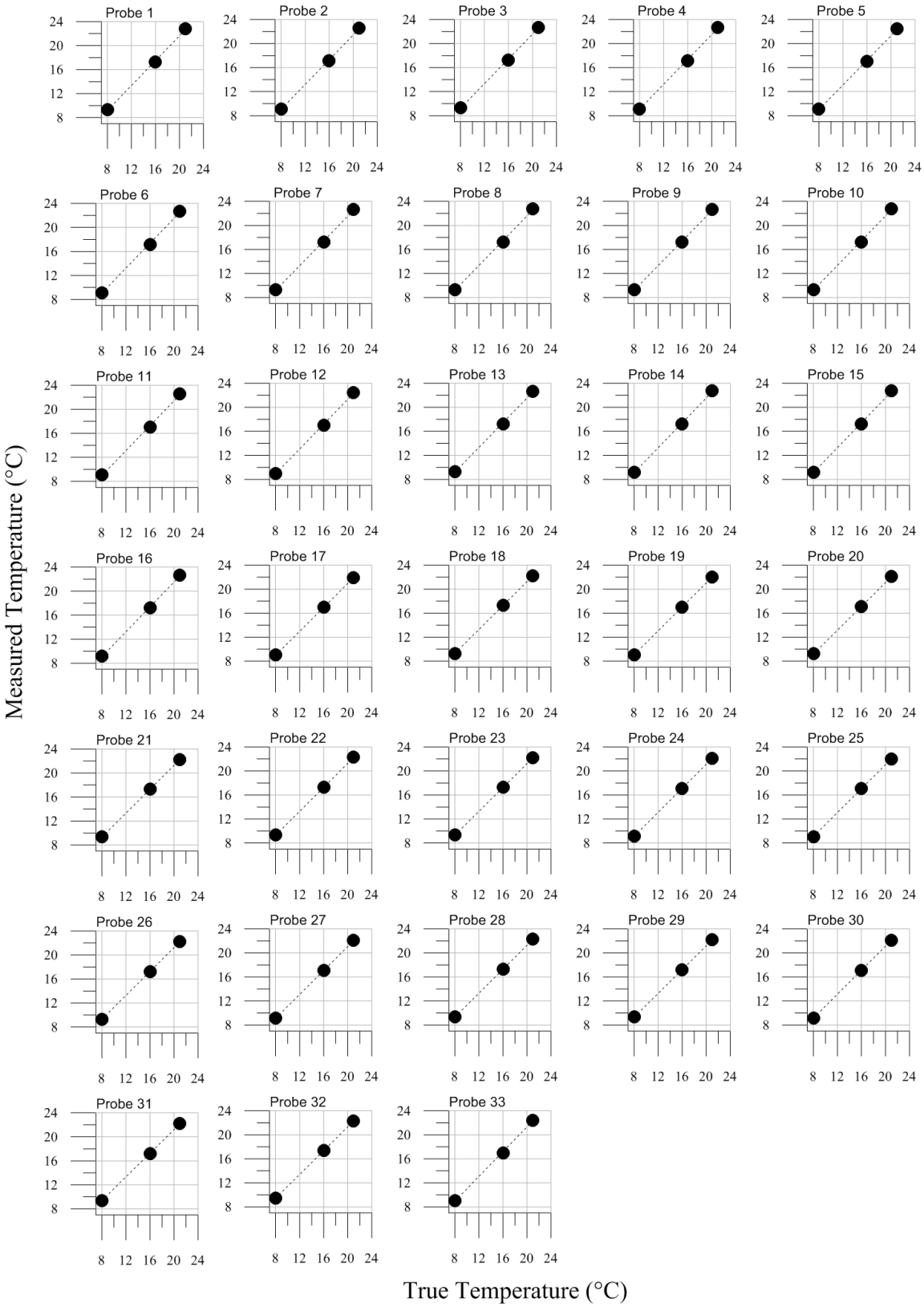

Figure A. 1: Calibration curves for all 32 temperature probe within the HI-RES TMD, and the surface water control probe (labelled Probe 33)

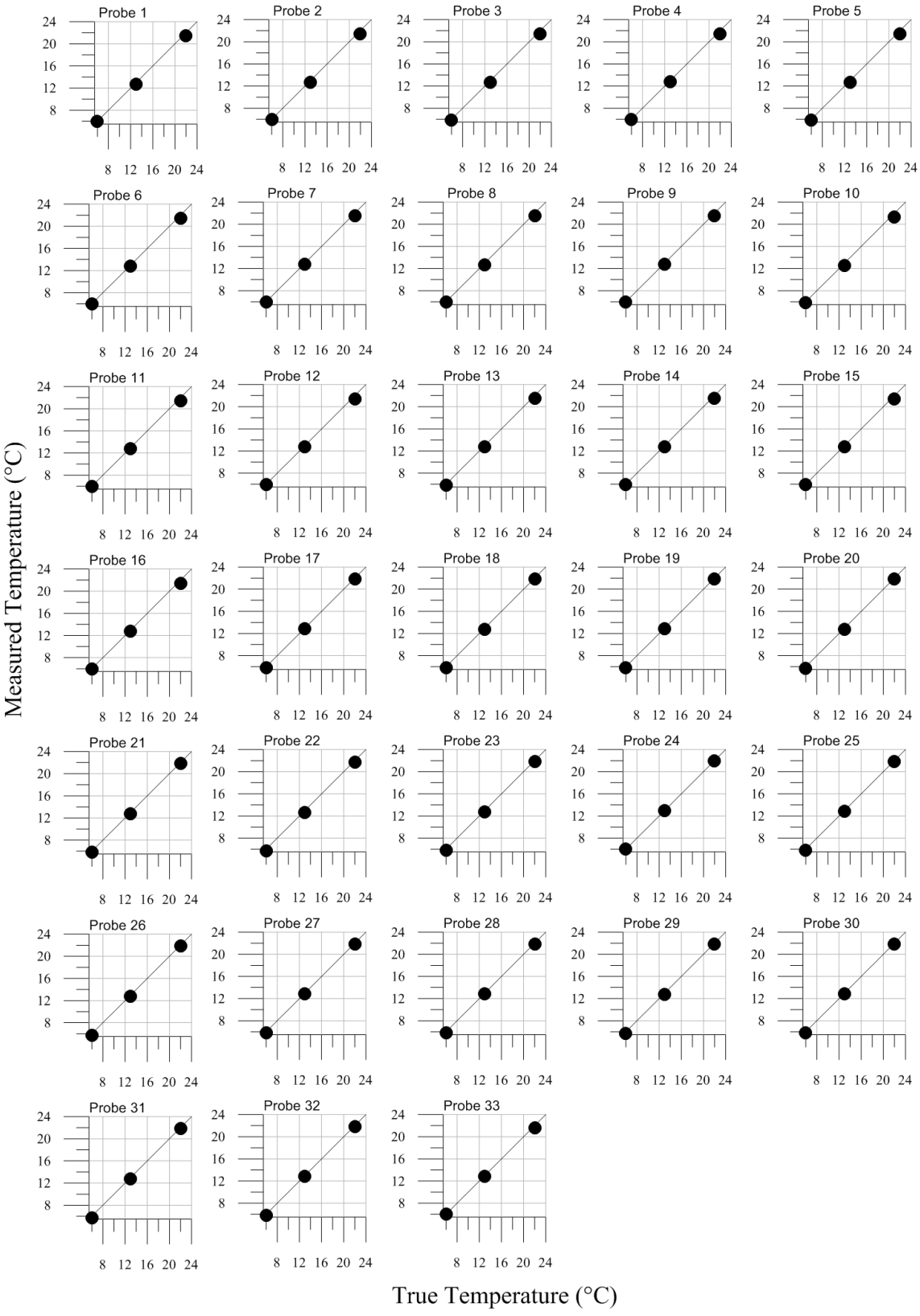

Figure A. 2: Validation curves for all 32 temperature probe within the HI-RES TMD, and the surface water control probe (labelled Probe 33)

Appendix B: Redd Survey Counts

Table B. 1: Summary of redds observed on Ram Creek

Feature[a]	Redd Counts			
	2012	2013	2014	TOTAL
Run 1	0	5	4	**9**
Pool 1	0	2	8[b]	**10**
Riffle 1	0	0	0	**0**
Run 2	10	0	4	**14**
Riffle 2	0	0	0	**0**
Pool 2	0	1	6[c]	**7**
Riffle 3	0	0	0	**0**
Run 3	0	6	7	**13**
Pool 3	0	2	3	**5**
Riffle 8	0	2	0	**2**
Pool 6	0	0	0	**0**
Riffle 7	0	0	2[d]	**2**
Run 5	0	0	0	**0**
Pool 7	0	0	0	**0**
Run 6	0	1	1	**2**
Pool 4	0	3	2	**5**
Riffle 6	0	0	0	**0**
Run 4	0	0	0	**0**
Riffle 5	0	0	0	**0**
Pool 5[e]	11	3	5	**19**
Run 7	0	1	0	**1**
Riffle 4	0	5	0	**5**
Run 8	10	15[f]	3	**28**
TOTAL	**31**	**46**	**45**	**122**

NOTES:

a. Features listed from upstream extent of the reach to the downstream extent. Indented feature represent by-pass channels
b. Area of spawning interest (AOI) represent a collection of redds that can't be differentiated because too many redds on top of one another. This AOI had approximately 7 redds and one other redd was identified within the feature.
c. One AOI with 4 redds and 2 separate redds within the feature
d. Cutthroat trout redds
e. Section of channel that migrated. In 2012, 9 redds are in the old channel, in 2013 3 redds in the old channel.
f. One AOI with 11 redds and 4 separate redds within the feature

Table B. 2: Summary of redds observed on Lizard Creek

Feature[a]	Redd Counts		
	2013	**2014**	**TOTAL**
Pool 1	0	0	**0**
Riffle 1	0	0	**0**
Run 1	0	0	**0**
Riffle 3	0	0	**0**
Run 3	0	0	**0**
Riffle 4	0	0	**0**
Run 4	0	0	**0**
Riffle 2	0	0	**0**
Run 2	3	1	**4**
Riffle 6	0	0	**0**
Pool 2	0	0	**0**
Riffle 7	0	0	**0**
Run 5	0	0	**0**
Pool 3	2	0	**2**
Run 6	0	0	**0**
Pool 4	0	2	**2**
Run 7	0	0	**0**
Riffle 8	0	0	**0**
Pool 5	1	2	**3**
Riffle 9	0	0	**0**
Run 8	1	3	**4**
TOTAL	**7**	**8**	**15**

NOTES:

a. Features listed from upstream extent of the reach to the downstream extent. Indented feature represent by-pass channels

Glossary

Alluvial Systems	River system in which the material constituting bed, banks and surroundings (valley side slopes, floodplain) is mobile sediment and soil
Bankfull depth	Distance from the lowest point in the cross-section and the top of the bank, measured vertically (perpendicularly from the channel bed)
Bankfull width	Width of the river measured from right to left bank, perpendicular to the flow direction
Cage	One single set of measurements completed with the HI-RES TMD, includes 32 streambed temperature measurements, 1 surface water temperature measurement ("control probe") and 1 pyranometer measurement
Cold spot	An area determined to be statistically significantly colder than its surroundings
D_{10}	10^{th} percentile of the grain size distribution curve representing the grain size for which 10% of the sample is smaller (10% of the sample is retained by the sieve)
D_{50}	Median of the grain size distribution curve representing the grain size for which 50% of the sample is smaller (50% of the sample is retained by the sieve).
D_{90}	90^{th} percentile of the grain size distribution curve representing the grain size for which 90% of the sample is smaller (90% of the sample is retained by the sieve)
Feature scaling	Data normalization done to reduce the range of values in the dataset
Glides	Downstream part of a pool, usually joining with a riffle and characterized by a negative (adverse, uphill) slope.
Grain size distribution curve	Graphical representation of the mass distribution of the particles sizes of the bed material.
Hot spot	An area determined to be statistically significantly warmer than its surroundings
Hyporheic flow	Subsurface (beneath the channel bed) flow occurring between water surface flow and the water table.
Isotherms	Thermal spatial contour map.
Left bank	The bank on the left side of the channel, defined as facing the downstream flow direction.
Longitudinal direction	Direction of flow in the river
Low-Flow	The lowest discharges (in magnitude) of the year. For Ram and Lizard creek this

	generally occurs in the winter and summer months
Morphological feature	A pool, a riffle or a run
Non-invasive	Any sampling technique not involving removal or movement of bed material from its original location.
Normalization	Process of removing underlying trends in the dataset
Pool	Deepest section of the river usually located between two riffles and characterized by flat water surface. Generally has finer sediment than riffles
Reach	Extended stretch along a river. Its boundaries can be arbitrarily defined although they usually coincide with specific morphological features.
Redd	Spawning site nest created by salmonids. It is created by the female salmonid laying on her side and digging a pit into the streambed.
Riffle	Shallow, fast water section of the river, characterized by larger sediments and steeper water surface and bed slope.
Right bank	The bank on the right side of the channel, defined as facing the downstream flow direction.
Riparian cover	Interface between land and a watercourse, often constituted by plants, it may cause localized shading on the channel bed
Run	Sections of the river slightly deeper and milder in depth than riffles but still characterized by fairly fast flow of water
Salmonids	Also known as *salmonidae*, family of ray finned fish of which trout, char and salmon are part of.
Significant Spots	General definition of a cold or hot spot
Sinuosity	Ratio of the river length divided by the valley length in which the latter is a straight distance from the upstream end to the downstream end of the reach.
Standardized temperature	Process creating a unitless temperature parameter
Streambed	The bottom of the river which creates the interface between the surface water and land.
Sub-reach	Subsection of a reach, in this document it generally regards a single pool-riffle sequence
Thermal capacity	Ratio of heat added to (or removed from) an object divided by the resulting temperature change. Generally measured in Joule per Kelvin.
Thalweg	Longitudinal path of the lowest points along the entire length of a streambed,

	defining its deepest channel.
Thiessen polygon	Partitioning of a plane surface in sub-areas based on the relative distance between points found on the surface itself.
Transverse direction	Direction perpendicular to the flow in the river (cross-sectional)